University of New Mexico
UNM Digital Repository

Earth and Planetary Sciences ETDs | Electronic Theses and Dissertations

11-13-1990

Geochemistry of Metal Segregation in Aubrites, and The Origin of Their Metallic Phases

Ignacio Casanova

Follow this and additional works at: https://digitalrepository.unm.edu/eps_etds

 Part of the Geology Commons

Recommended Citation
Casanova, Ignacio. "Geochemistry of Metal Segregation in Aubrites, and The Origin of Their Metallic Phases." (1990).
https://digitalrepository.unm.edu/eps_etds/241

This Dissertation is brought to you for free and open access by the Electronic Theses and Dissertations at UNM Digital Repository. It has been accepted for inclusion in Earth and Planetary Sciences ETDs by an authorized administrator of UNM Digital Repository. For more information, please contact disc@unm.edu.

UNIVERSITY OF NEW MEXICO
A14412 315935

GEOCHEMISTRY OF METAL SEGREGATION IN AUBRITES, AND
THE ORIGIN OF THEIR METALLIC PHASES - CASANOVA

ZIM
LD
3783
G46
1990
C37

A14412 315935

DATE DUE

APR 27 1994

APR 18 1997

APR 18 2000

AUG 28 2010

DEMCO 38-297

ZIM
LD
3783
G46
1990
C37

THE UNIVERSITY OF NEW MEXICO
ALBUQUERQUE, NEW MEXICO 87131

POLICY ON USE OF THESES AND DISSERTATIONS

Unpublished theses and dissertations accepted for master's and doctor's degrees and deposited in the University of New Mexico Library are open to the public for inspection and reference work. *They are to be used only with due regard to the rights of the authors.* The work of other authors should always be given full credit. Avoid quoting in amounts, over and beyond scholarly needs, such as might impair or destroy the property rights and financial benefits of another author.

To afford reasonable safeguards to authors, and consistent with the above principles, anyone quoting from theses and dissertations must observe the following conditions:

1. Direct quotations during the first two years after completion may be made only with the written permission of the author.

2. After a lapse of two years, theses and dissertations may be quoted without specific prior permission in works of original scholarship provided appropriate credit is given in the case of each quotation.

3. Quotations that are complete units in themselves (e.g., complete chapters or sections) in whatever form they may be reproduced and quotations of whatever length presented as primary material for their own sake (as in anthologies or books of reading) ALWAYS require consent of the authors.

4. The quoting author is responsible for determining "fair use" of material he uses.

This thesis/dissertation by Ignacio Casanova has been used by the following persons whose signatures attest their acceptance of the above conditions. (A library which borrows this thesis/dissertation for use by its patrons is expected to secure the signature of each user.)

NAME AND ADDRESS	DATE

Ignacio Casanova

Candidate

Geology

Department

This dissertation is approved, and it is acceptable in quality and form for publication on microfilm:

Approved by the Dissertation Committee:

, Chairperson

Accepted:

Asst. *Dean, Graduate School*

November 13, 1990

Date

GEOCHEMISTRY OF METAL SEGREGATION IN AUBRITES, AND THE ORIGIN OF THEIR METALLIC PHASES

BY

IGNACIO CASANOVA

B.S. Geology, University of Barcelona (Spain), 1986

M.S. Geology, University of Barcelona (Spain), 1988

DISSERTATION

Submitted in Partial Fulfillment of the
Requirements for the Degree of

Doctor of Philosophy in Geology
The University of New Mexico
Albuquerque, New Mexico

December, 1990

© Copyright by Ignacio Casanova, 1990

DEDICATION

To my wife, sister and father,

and very especially to my mother, *in memoriam*.

ACKNOWLEDGEMENTS

Many people have contributed to this work achieving its final form.

Professor Alfredo San Miguel introduced me to the exciting field of Planetary Geology, and taught me many things that cannot be found in books. Thank you, Alfredo.

I thank the members of my committee, Professor K. Keil, Dr. H.E. Newsom, Professor J.J. Papike, Professor C.J. Yapp, and Professor D.G. Brookins for their comments and suggestions which greatly improved the original form of the manuscript.

I also wish to express my deepest gratitude to all the members of the Spanish Association of Planetary Studies. They have provided a great deal of encouragement and support, and keep on working for the development of Planetary Science in Spain.

Professor G.J. Taylor made essential contributions through many discussions about the complexity and interest of the study of the magmatic evolution of asteroids. Professor A.M. Kudo helped me understand many concepts of chemical equilibrium of unusual mineral assemblages. Professor Carlos Bustamante taught me about the universality of Physical Chemistry. Alejandro Gonzalez-Aller was always ready to discuss the mathematical treatment.

I had numerous and valuable discussions with Ms. Maya Wheelock which gave me a more complete picture of aubrite magmatic evolution; we also shared many of the problems that make the study of aubrites a challenging task. Mr. Timothy J. McCoy reminded me many times that there is a lot to know about meteorites before they become molten.

My thanks to Mr. George Conrad for keeping the microprobe lab running and spending a lot of time training me on microprobe analysis. To Mr. Tom Servilla for excellent and prompt preparation of the samples. To Mr. Ken Nichols for preparation of very high quality photographic material. To Mr. Troy Beserra for his constancy and ability in the maintenance of the instrumental neutron activation lab. And, to all the personnel of the Institute of Meteoritics, who without exception provided the necessary strategic and scientific support for the completion of this work.

This work was partially supported by the National Aeronautic and Space Administration grants NAG 9-30 and NAG 9-454 (K. Keil, principal investigator), and the National Science Foundation grant EAR 8804070 (H.E. Newsom, principal investigator). Financial support from the Institute of Meteoritics (J.J. Papike, Director) is also gratefully acknowledged.

GEOCHEMISTRY OF METAL SEGREGATION IN AUBRITES, AND THE ORIGIN OF THEIR METALLIC PHASES

BY

IGNACIO CASANOVA

B.S. Geology, University of Barcelona (Spain), 1986

M.S. Geology, University of Barcelona (Spain), 1988

ABSTRACT OF DISSERTATION

Submitted in Partial Fulfillment of the
Requirements for the Degree of

Doctor of Philosophy in Geology

The University of New Mexico
Albuquerque, New Mexico

December, 1990

GEOCHEMISTRY OF METAL SEGREGATION IN AUBRITES AND THE ORIGIN OF THEIR METALLIC PHASES

Ignacio Casanova

B.S. Geology, University of Barcelona (Spain), 1986
M.S. Geology, University of Barcelona (Spain), 1988
Ph.D. Geology, University of New Mexico, 1990

Aubrites are highly reduced igneous meteorites consisting of nearly FeO-free silicates and minor (<0.5-5 wt.%) amounts of Si-bearing metallic Fe,Ni. This study provides the first systematic chemical characterizationof the metal phases present in aubrites, with the aim to constrain ideas about the thermal history and origin of aubritic metal. The apparent metallographic cooling rates may be too low by a factor of 6 to 15 due to the presence of significant amounts (a few tenths of a percent) of Si and P in the metal. The distribution of siderophile elements between the silicates and Fe,Ni is consistent with that expected from metal segregation occurring upon melting of an enstatite chondrite-like material, but calculations on the amount of metal involved in the differentiation process are unconstrained due to uncertainties on silicate/metal partition coefficients of siderophile elements under highly reducing conditions. The approximately chondritic values of siderophile element contents in the metal indicate that the analyzed metallic particles are not fragments of a fractionally crystallized Fe,Ni core. Therefore, these particles probably represent material that was trapped in the silicate magma as a result of inefficient core formation. Model calculations suggest that the variability of Si contents found among metal particles may be due to local equilibrium conditions (*i.e.*, variable oxygen fugacities), resulting from compositional heterogeneities of the precursor material.

TABLE OF CONTENTS

LIST OF FIGURES

Page

LIST OF TABLES

1. INTRODUCTION

Enstatite achondrites, also called aubrites, are differentiated stone meteorites largely made up of nearly FeO-free enstatite and contain a variety of rare minerals formed under the most reducing conditions recorded in solar system materials (e.g. Keil and Fredriksson, 1963; Keil and Brett, 1974; Watters and Prinz, 1979; Brett and Keil, 1987; Keil, 1989). Although some authors have suggested a direct nebular condensation origin for aubrites (Wasson and Wai, 1970; Richter *et al*., 1979; Sears, 1980), there is now strong evidence that these meteorites are the products of igneous processes in their parent body or bodies. The evidence consists of the following:

(a) Clasts in brecciated aubrites display unequivocal igneous textures, suggesting crystallization from silicate magmas (e.g. Okada *et al*., 1988)

(b) Aubrites generally contain large crystals of enstatite (up to 8 cm in Norton County). It is very unlikely that crystals of such size can grow as a result of the rapid cooling expected to occur in a condensation process (Okada *et al*., 1988).

(c) There is a correlation between non-volatile and volatile siderophiles (Ir, Os, Re, Pd, Ni with Ge) and incompatibles (U, REE and Cs; Wolf *et al*., 1983). Such correlations are also seen in basaltic achondrites and lunar rocks; it is doubtful whether they can be produced by nebular processes.

(d) The rare earth abundance patterns show fractionated trends (e.g. Graham and Henderson, 1985). If aubrites formed by condensation, the observed negative Eu anomalies should be accompanied by similar depletions of Yb (which are not observed in aubrites), since fractionation would then be governed by volatility (Eu and Yb are the two most volatile REE). Although we know very little about the behavior of REE under such low oxygen fugacity conditions, it is reasonable to assume that Eu has been removed by the crystallization of a Ca-rich phase (not necessarily plagioclase; in this case, oldhamite, CaS, may have played an important role), but this has not been unequivocally proven so far. However, if as suggested by Floss *et al.* (1990), the REE contents in oldhamite are relict, the distribution patterns of these elements displayed in this sulfide phase (Wheelock *et al.*, 1989) may not be good indicators of igneous processes.

The study of aubritic metal can provide important clues about the origin and igneous and metamorphic history of the enstatite achondrite parent body. In this work, I have carried out a petrographic and geochemical study of the metallic particles present in aubrites with the aim of constraining ideas about their origin and evolution. The extremely low oxygen fugacities under which enstatite meteorites formed (e.g. Larimer and Buseck, 1974; Fogel *et al.*, 1989) and their consequent unique composition make interpretations difficult due to the lack of experimental data on highly reducing systems. I have tried to overcome the paucity of experimental data by using a theoretical

thermodynamic approach to study the significance of such unique compositions based on three main themes: (1) the conditions of formation of the high-Si Fe,Ni alloys found in aubrites, (2) the study of the partitioning behavior of siderophile elements and their abundances relative to chondritic metal, and (3) the significance of perryite formation, which is unique to enstatite meteorites.

Although it does not give definitive answers to the problem of the origin of the metal in aubrites and its thermal history, the present work provides several working hypotheses which constrain previous ideas on aubrite evolution. These hypotheses can be summarized into three main lines of thought:

(1) The petrology and chemical composition of aubrites suggest a complex (multi-stage) thermal history during which several magmatic and/or metamorphic reheating events may have operated.

(2) The metal particles of known aubrites are not fragments of a fractionally crystallized Fe,Ni core from their parent body. This work suggests that the metal represents trapped, disseminated globules that did not efficiently sink in a parent silicate magma.

(3) The siderophile element signatures of aubritic silicates is consistent with the melting of a precursor material in principle similar to enstatite chondrites but with substantially lower amounts of metal. This idea supports previous works that suggest that known enstatite

chondrites are not the precursors of aubrites (e.g. Brett and Keil, 1987; Keil, 1989). A high degree of partial melting of such precursor material is required to account for the observed siderophile element pattern in the silicates.

2. PREVIOUS WORK

In spite of the extensive literature on enstatite meteorites (e.g. Keil, 1989, and references therein), studies on aubritic metal are scarce. The early work by Wai (1970) and Wasson and Wai (1970) provided a basic characterization of the chemical composition of the metallic phases present in aubrites and the related meteorites Mount Egerton and Horse Creek. The above mentioned authors proposed the existence of a compositional trend among aubrites and suggested a similar origin for the enstatite meteorites (chondrites and achondrites) on the basis of the existence of metallic inclusions in the enstatite which, according to their interpretation, argued against an igneous origin for aubrites. Newsom and Drake (1979) addressed the problem of the origin of the metal clasts in Bencubbin, an anomalous enstatite-rich achondritic breccia that might be related to the aubrites, and favored an equilibrium condensation hypothesis. Later studies by Watters and Prinz (1979, 1980) suggested the possibility that the reduced Si-bearing metal-rich meteorites Horse Creek (anomalous iron) and Mt. Egerton (anomalous stony-iron) represent the differentiated core of an enstatite meteorite parent body in which aubrites formed the mantle. Wolf *et al.* (1983) carried out the first extensive trace element study of aubrites and obtained data on the metallic fractions in Mayo Belwa and Mt. Egerton. They distinguished two types of aubritic metal on the basis of the siderophile element abundance patterns that they believe reflect a combination of several nebular and igneous processes. Ntaflos *et al.* (1988) also suggested the existence of at least two populations (Si-rich and Si-poor) in the metal fraction of Khor Temiki. Finally, Casanova *et al.* (1990) initiated a systematic study of aubritic metal, providing

major, minor and trace-element characterization of Norton County metal nodules. They suggested that the metal particles are trapped objects from inefficient core formation (metal segregation) in the aubrite parent body, as opposed to pieces of a fractionally crystallized metallic Fe,Ni core.

Some key unsolved questions remain to be answered regarding the problem of the origin and evolution of the metal phase in aubrites and, by extension, the aubrite parent body. Some of these questions, which are addressed in this work, are common to the more general problems of meteorite study, and include (1) the source of the metal (indigenous or foreign), (2) the extent of metal segregation in differentiated meteorites, (3) the starting composition and characteristics of the precursor material, (4) the number of parent bodies from which the aubrites originated, (5) the pressure and temperature conditions, the composition, and the duration of asteroidal magmatic episodes, and (6) the nature of the heat sources that operated in the early history of the solar system.

3. SAMPLES AND METHODS

Cut and/or broken surfaces of available meteorites were examined visually and with a low-power stereomicroscope in order to identify metal inclusions, or any other features worthy of detailed study; the main mass of Norton County (1 ton, collection of the Institute of Meteoritics) was also examined visually. Petrographic observations were carried out in reflected light on polished sections (Table 1), mildly etched with nitol (a dilute solution of HNO_3 in ethyl alcohol). Modal analyses of polished sections were made by point counting for metallic Fe,Ni.

Fe,Ni, schreibersite and perryite were analyzed for Fe, Ni, Co, Si, P and Cr using an ARL EMX electron microprobe operated at an accelerating voltage of 15 kV and approximately 20 nA beam current. Standarization was carried out with pure elements for Fe, Ni and Co. A Fe_3Si alloy was used for the analysis of Si, and a well-characterized schreibersite grain from Norton County served as the P standard; its P concentration was calculated from the stoichiometric formula $(Fe,Ni,Co)_3(P,Si)$ for known Fe, Ni, Co and Si concentrations determined by microprobe. Interference of the Co K_α line by the Fe K_β line was corrected for by measuring Co in our pure Fe standard and substracting the corresponding amount from each analysis in proportion to its Fe concentration. Microprobe mineral analyses were corrected using ZAF correction procedures. Bulk analyses of metallic particles were performed using a broad beam of variable diameter (depending on the dimensions of each grain analyzed) and averaging the results; for particles of <20 μm in maximum dimension, point analyses were used

Meteorite	Section Nos.	Source
ALHA 78113	10, 19, 22, 53, 61	MWG
ALH 84007*	4, 38, 59	MWG
ALH 84008*	4, 66	MWG
ALH 84009*	4, 9	MWG
ALH 84010*	4, 5	MWG
ALH 84011*	5, 30	MWG
ALH 84012*	5	MWG
ALH 84013*	5	MWG
ALH 84014*	3	MWG
ALH 84015*	5	MWG
ALH 84016*	7	MWG
ALH 84017*	5	MWG
ALH 84018*	3	MWG
ALH 84019*	3	MWG
ALH 84020*	5	MWG
ALH 84021*	2	MWG
ALH 84023*	8	MWG
ALH 84024*	8	MWG
Aubres	63552	BM
Bishopville	222-1	USNM
Bustee	32100	BM
Khor Temiki	1934, 781a (P 205, 238)	BM
Mayo Belwa	1336, 1371	BM
Mount Egerton	3271-1, 3271-2	USNM
Norton County	483A, 528, 529, 538, 576, 812, 915, 916, 923, 932, 933, 934, 935, 936, 950, 952, 961, 962	UNM

TABLE 1.- Polished sections of aubrites studied in this work. Samples marked with an asterisk are paired. Source key: MWG - Meteorite Working Group, Johnson Space Center; BM - British Museum; USNM - U. S. National Museum; UNM - University of New Mexico.

to calculate the bulk composition. For grains of <10 μm in maximum dimension, possible contamination of Si from the surrounding silicates was monitored by analyzing Mg simultaneously; analyses with detectable amounts of this element were rejected.

For neutron activation analysis, metal inclusions of sizes ranging between 0.3 and 1.5 cm in maximum dimension were removed from their silicate hosts, and cut into two pieces (when possible) with a diamond wire saw in order to preserve some material for additional petrographic study. Silicate material and rust were ground from the metal with a dental drill, using a tungsten carbide tip. Cut pieces of the Filomena specimen of the North Chile hexahedrite were used as a primary standard for the determination of Co, Ni, Ga, W, Re, Ir, and Au, and as a secondary standard for Cr, and As. The NBS steel 809b (also marketed in different size as 409b) is the nearest to an iron meteorite in composition. Because of its high and uniform concentrations of siderophile elements, it was used as a primary standard for Cr, As, and Sb, and as secondary standard for Co, Ni, Ga, W, and Au. Additional secondary standards for W and Re were prepared by evaporating certified monitor solutions of these two elements in an ultrapure Fe powder matrix. This powder was previously analyzed to confirm that concentrations of these elements were below the detection limit of the INAA technique. Clean metal samples and standards were then lightly etched in a 15% HNO_3 solution (except the standards prepared from monitor solutions), rinsed in acetone, dried, weighed, and packaged in snap-top polyethylene vials. Irradiations were carried out in Port 4 of the Omega West Reactor at Los Alamos National Laboratories during 20 minutes at a thermal neutron flux of approximately

10^{13} neutrons cm^{-2} s^{-1}. The γ-ray counting was performed on a Ge(Li) coaxial detector and the pulses recorded on a 4096-channel analyzer. Two different detectors with efficiencies of 22.1% and 15% and peak-to-compton ratios of 52.1:1 and 36:1, respectively, were used during the course of this work. Each sample was counted four times over a period of three weeks. The γ-ray spectra were processed and reduced using interactive software developed by Kruse (1979) and Kruse and Spettel (1982).

4. PETROGRAPHY

4.1. Fe,Ni

Fe,Ni in aubrites occurs as 1) small inclusions in enstatite, 2) irregularly-shaped masses of up to a few hundreds of microns, 3) large metal nuggets, and 4) submicron-sized blebs, finely dispersed in the silicates as a result of shock melting. Some of these petrographic types are shown in Figs. 1 and 2.

The small metallic inclusions in enstatite are only a few microns in maximum dimension and their grain distribution is generally parallel to the direction of cleavage of the host crystal (Fig. 2A). They usually have euhedral shapes, although rounded blebs are also common. There is no apparent relationship between the size of the enstatite host and the number or shape of the metallic inclusions it contains.

The large metal nodules are usually well-rounded, polycrystalline masses of kamacite (Fig. 1), although cm-sized single crystals of this mineral also exist. They vary in size from approximately 2 mm to 1.5 cm in diameter. Inclusions of sulfides and silicates are rare and tend to be concentrated on the borders of the nodule. Metal-metal grain boundaries are visible upon etching and serve as preferred nucleation sites for schreibersite and/or perryite. Only some of the larger metal nuggets (> 0.5 cm in diameter) display perryite exsolution.

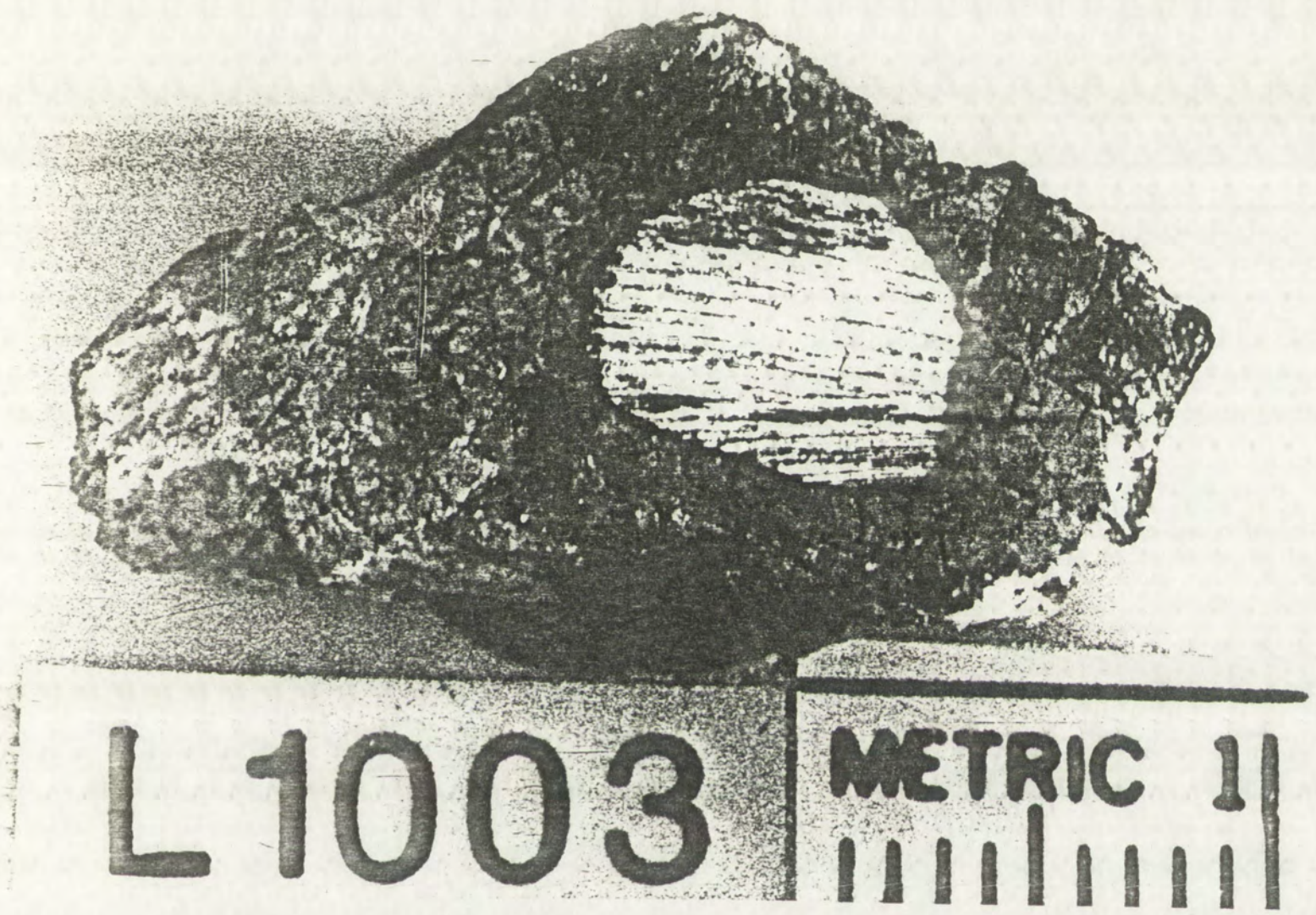

FIGURE 1.- Metal nodule in Norton County. Scale is 1 cm; small divisions are 1 mm.

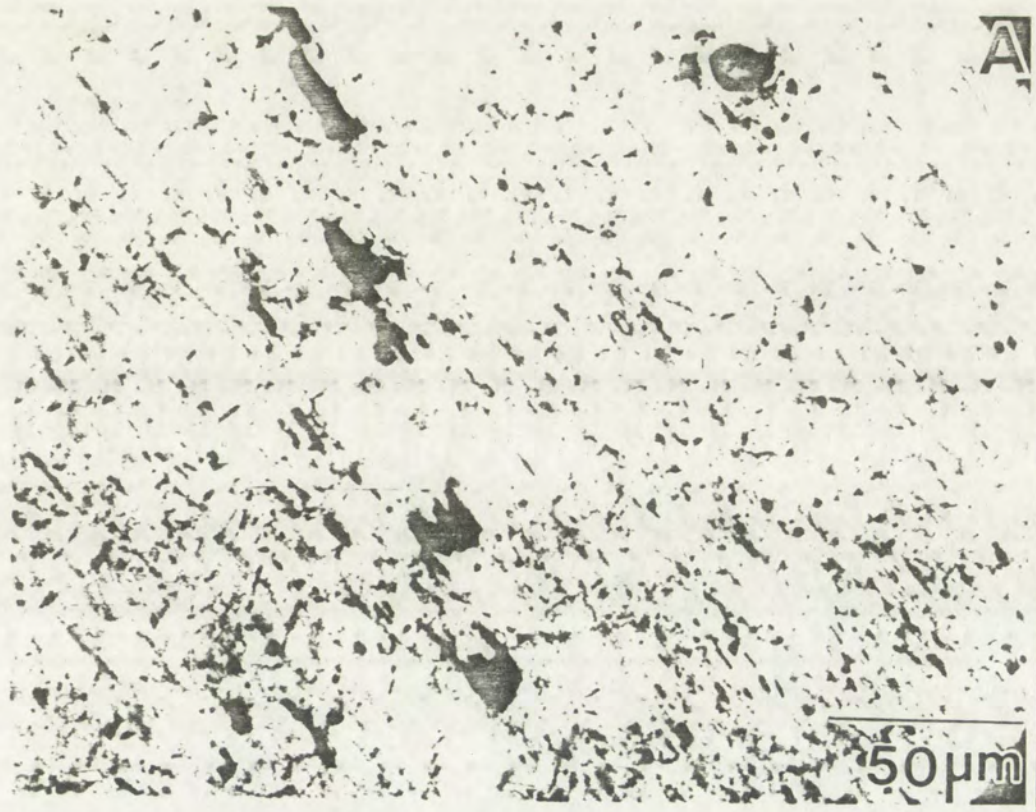

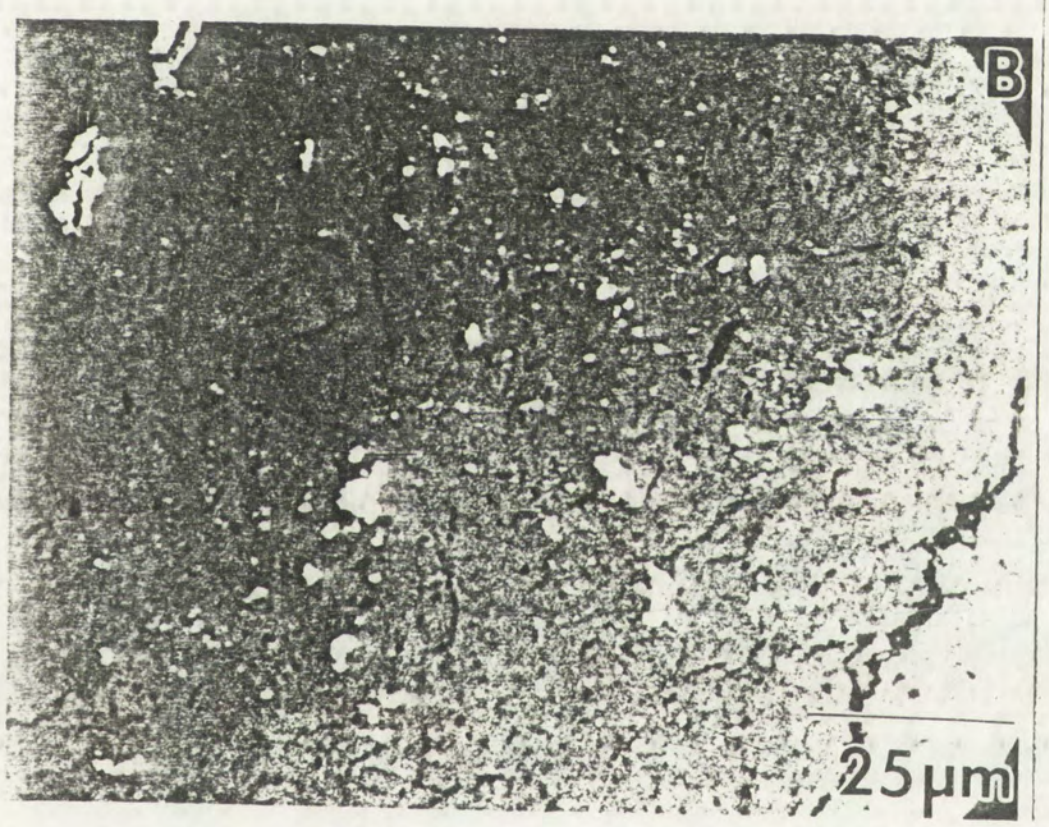

FIGURE 2.- (A) Small metallic inclusions (dark) oriented parallel to the direction of cleavage of the enstatite; transmitted light. (B) Shock-melted, finely dispersed metal in silicate host; reflected light.

Metal in aubrites is low in abundance. A modal analysis of approximately 35000 points carried out on twelve polished thin sections of Norton County yields a metal content of about 1 vol.%; however, this is has to be considered as a lower limit since the large metal nodules are not represented in the studied sections. To solve this sampling problem (at least partially), point counting for metal grains larger than 2 mm in size was carried out on a 30x14 cm sawed specimen of Norton County; this procedure yielded a value of approximately 0.3 vol.%. This result indicates that the actual metal content of Norton County must be 1-1.5 vol.%, a little higher than that reported by Okada *et al.* (1988).

The abundance of metal in Norton County is heterogeneous on a centimeter scale. This was evidenced after a careful examination of the main mass (1 ton) of this meteorite, which displays areas of variable sizes (generally of a few centimeters) where metal content (as evidenced by reddish weathering aureoles) is clearly higher than in others, which have the uniform whitish coloration typical of enstatite. Additional modal analyses of the thin sections listed in Table 1 reveal that the metal content in aubrites is quite variable (0.1-2.3 vol.%), confirming the heterogeneous distribution observed in Norton County. Anyhow, the metal abundance in aubrites is clearly very low. Models of possible precursor materials that melted to form aubrites must explain this fact.

Shock features in kamacite are difficult to distinguish in the meteorites studied in this work. Only three metal grains of a few tens of microns in maximum dimension from ALH 84007 display a characteristic mosaic stucture.

It is likely that this feature correponds to "Case 3" of the shock effects in metallic phases of meteorites discussed by Stoffler *et al.* (1988). This is a situation where the shock wave is attenuated by internal cracks and inclusions, resulting in strong post-shock heating and significant plastic deformation; the fine-grained kamacite may start recrystallizing due to the residual heat and end up forming the observed microstructure. It is difficult to decide, solely on the basis of petrographic studies, whether the different degrees of shock displayed in a single rock are due to mixing of components which experienced different shock histories, or just differential propagation of shock waves in a texturally heterogeneous material. However, the proximity of metal and silicate grains with substantially different shock features makes the mixing possibility more likely.

4.2. Schreibersite

Schreibersite [$(Fe,Ni,Co)_3(P,Si)$] in the studied aubrites is associated with metal grains, except in a few cases where it occurs isolated as an accessory component in the clastic matrix material. In this work, at least four different morphological varieties of schreibersite have been observed: large vermicular grains, "rhabdite", anhedral or subhedral equidimensional crystals, and needles.

Vermicular schreibersite occurs at grain boundaries between kamacite crystals in a single metal inclusion (Fig. 3B). It appears as elongated crystals of up to 2.5 mm in length by a few tens of microns in width, which broaden to form more massive crystals near the edges of

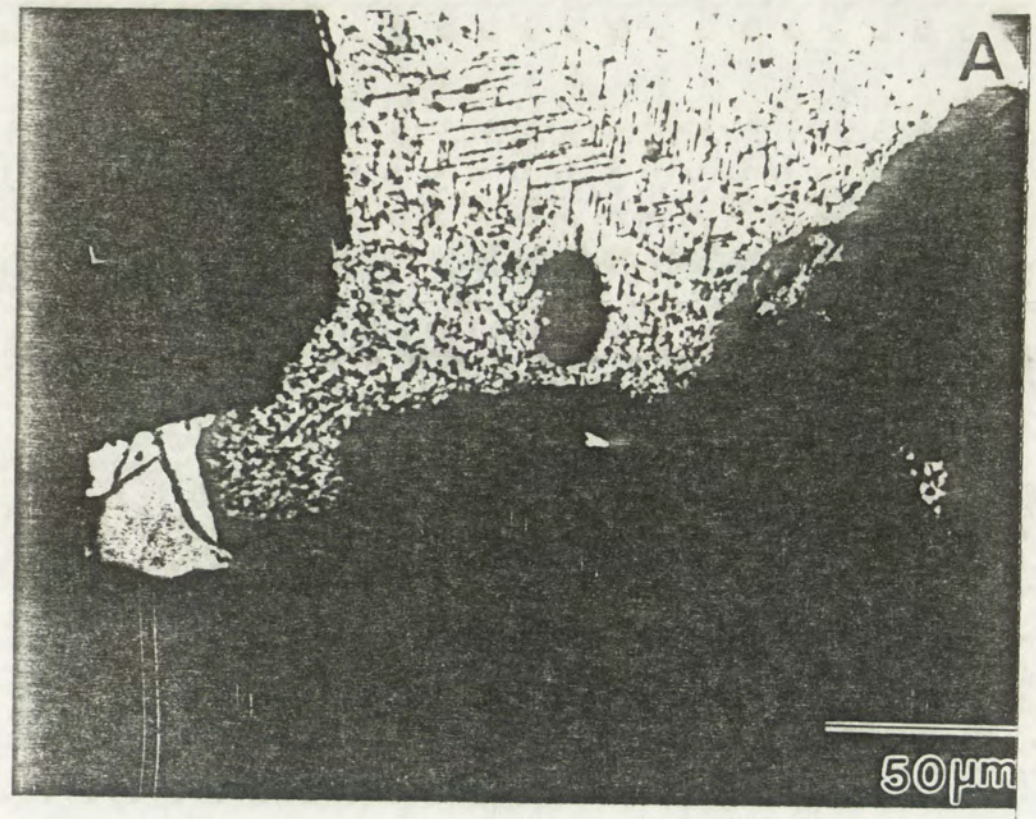

FIGURE 3.- (A) Igneous metal-silicate contact in Norton County. Exsolution lamellae in the metal are perryite. The brighter grain at the lower left interface is schreibersite. Etched. Reflected light. (B) Vermicular schreibersite in perryite-bearing kamacite host. Etched. Reflected light.

the inclusion (i.e., the metal-silicate grain boundaries). Cleavage perpendicular to the direction of maximum elongation is common, especially in the larger crystals.

The rhabdite variety of schreibersite has been found in this work in only one metal grain of the Antarctic aubrite ALHA 78113 (section 78113, 53). Rhabdites occur as small, euhedral grains of sizes ranging between approximately 5 and 50 microns, and grow in the center of the metal inclusion.

Equidimensional schreibersite grains nucleate preferentially at metal-silicate and metal-sulfide interfaces and tend to be more euhedral towards the interior of the kamacite host (Fig. 3A). They are variable in shape and size (10-700 μm). They can also form at boundaries between different kamacite grains in a single metal inclusion; in these cases, they appear as discontinuous trails of grains of a few microns in size.

Schreibersite needles grow in the interior of Fe,Ni inclusions. They are lens-shaped grains of sizes not exceeding a few tens of microns in length and 1-5 microns in width. Such needles show preferred orientations parallel to the (111) planes of the kamacite host; this orientation was determined using the method described by Buchwald (1969).

The abundance of schreibersite is difficult to determine because grains of this mineral are very heterogeneously distributed and often have irregular shapes and highly variable sizes within a single metal inclusion. A modal analysis of two polycrystalline metal nodules in Norton County (with diameters

of 1.5 and 0.8 cm) reveal that schreibersite can constitute up to approximately 6 vol.% of the metal inclusion.

4.3. Perryite

Perryite is a nickel silicide containing minor amounts of phosphorous and iron and trace amounts of cobalt. It usually occurs as thin rims and lamellae around and within kamacite grains of enstatite meteorites and in an unusual iron meteorite, Horse Creek. The mineral was first described by Ramdohr (1963), and Fredriksson and Henderson (1965) provided the first chemical analysis. Based on a detailed crystallographic study, Okada *et al.* (1987) proposed a structural formula $(Ni,Fe)_8(Si,P)_3$.

In this work perryite has only been identified in the Mt. Egerton and Norton County meteorites. Its presence is revealed upon etching with nitol, and it appears as a pale yellow-colored mineral. In aubrites, perryite generally occurs as lamellae of up to several millimeters in length and about 5-30 microns in width, parallel to the (111) directions of the kamacite crystal. The lamellae generally display submicron inclusions of a darker coloration, which might represent another phase.

Perryite also appears as small anhedral grains of a few microns in maximum dimension which have nucleated preferentially at metal-silicate and metal-metal grain boundaries, forming in some cases discontinuous rims. Modal analyses of four Norton County and two Mt. Egerton perryite-bearing metal nuggets reveal that the abundance of this mineral is essentially the same

in the studied metal nodules of both meteorites (1.5-2.0 vol.%). It is also important to note that perryite in aubrites occurs exclusively in large, centimeter-sized metal nodules, and that the smaller metal particles are devoid of it.

Differerent degrees of recrystallization have been observed in Norton County perryites (Fig. 4). Recrystallization causes broadening and anhedralization of the lamellar crystals, producing a characteristic texture which is essentially identical to that observed in the Horse Creek hexahedrite by Buchwald (1975). Such textural characteristic has been interpreted as a result of a reheating episode where temperatures on the order of 1300 C were briefly exceeded (Buchwald, op. cit.). In addition to this feature, the Norton County perryite lamellae show distinctive shock features, including plastic deformation, kinks, and small displacement fractures. However, perryites in the two Mt. Egerton metal nodules studied in this work do not display any appreciable evidence of recrystallization or shock effects.

4.4 Textural relationships

4.4.1. Metal-silicates and sulfides

Two different types of metal-silicate textural relationships can be established on the basis of the observed contacts among grains: (a) igneous contacts, evidenced by smooth interfaces and euhedral to subhedral inclusions of silicate material (mostly enstatite) in metal particles, and (b) breccia contacts, which show characteristic angular grain boundaries of

FIGURE 4.- Unrecrystallized (A) and recrystallized (B) perryite exsolution lamellae in two different metal nodules of Norton County. Etched. Reflected light.

metallic particles embedded in finely comminuted silicate material. Igneous contacts are more common between big metal nuggets and their silicate surroundings. The existence of micron to sub-micron sized particles of metal which are generally oriented parallel to main cleavage directions in large enstatite crystals is also interpreted as being a result of coexistence of molten material. An exsolution origin for these small particles can be in principle ruled out on the basis of their relatively high-Ni contents. On the other hand, breccia contacts are more common among the fine-grained fraction of metal which appears in the aubrite matrix material.

Mt. Egerton is unbrecciated and it displays the most clear-cut metal-silicate igneous contacts among enstatite meteorites. In Mt. Egerton, Fe,Ni and silicates are intergrown showing euhedral grains of enstatite in the interior of the metal (e.g. McCall, 1965), evidence of the earlier crystallization of the silicate component.

Sulfides in aubrites are found in a variety of parageneses, occurring as well-rounded inclusions in kamacite, on metal-silicate grain boundaries, and as complex polycrystalline nodules. Detailed descriptions of aubritic sulfides are given by Wheelock et al. (1989) and Wheelock (1990).

4.4.2. Schreibersite-perryite

The few observed perryite-bearing metal nodules, without exception, contain a certain amount of schreibersite. The crystallization of the anhedral masses of schreibersite predates, in all cases, the nucleation of perryite. This

is evidenced by the existence of nickel-depleted rims, of a few microns in width, around schreibersite crystals (Fig. 3B). The extraction of Ni caused by the crystallization of schreibersite prevents the exsolution of perryite lamellae parallel to the (111) planes of the kamacite. This exsolution is likely to represent a late event in the sub-solidus cooling history of aubritic metal, as will be discussed in a following section.

Schreibersite needles have been identified in only one metal nodule, of 0.7 cm in diameter (Norton County, section UNM 576). These needles display the same orientation as the more abundant perryite lamellae, although the textural relationship between both phases is obscured by an alteration rim around the schreibersite. The observed orientation might be indicative of simultaneous exsolution of perryite and schreibersite needles.

It is difficult to establish a chronological sequence in the crystallization of the different varieties of perryite (i.e., anhedral and lamellae) solely on the basis of textures. However, the fact that anhedral perryite grains tend to nucleate at or in the proximity of grain boundaries (heterogeneous nucleation) suggests that irregular perryites crystallized immediately before, or simultaneously with, the lamellae.

5. CHEMICAL COMPOSITION

5.1 Major and minor elements

5.1.1. Fe,Ni

I have measured the contents of Fe, Ni, Co, Si, P and Cr in 215 metal grains of eight different aubrites and Mt. Egerton. Cr was below detection limit (0.08 wt.%) in all cases. A summary of the compositional range of the kamacite of the studied meteorites is given in table 2. Additional data on aubritic metal composition are given by Wai (1970), Wasson and Wai (1970), Graham (1978), Watters and Prinz (1979), Easton (1986), Ntaflos *et al.* (1988), Okada *et al.* (1988), and Keil (1989).

Phosphorous has been found to be very close to or below detection (0.02 wt.%) in all the analyzed grains except for Khor Temiki (P=0.08-0.13 wt.%), Mayo Belwa (P= <0.02-0.25 wt.%), one 4-mm metal particle in ALHA 78113 (P=0.11 wt.%), and one 0.5-mm inclusion in Norton County (P=0.69 wt.%).

Cobalt contents show different degrees of variability from meteorite to meteorite. Thus, while the compositions of ALH 84007, Aubres, Bustee and Khor Temiki are relatively constant (0.23-0.37 wt.% Co), other aubrites show much larger variations (e.g., 0.09-0.56 wt.% Co in Mayo Belwa). Higher compositional variation for Co corresponds in all the studied meteorites to an

TABLE 2.- Compositional range of kamacite in aubrites.

Meteorite	Size range (μm)	Si	P	Fe	Co	Ni	No. of grains
ALHA 78113	20 - 4000	0.03 - 0.29	< 0.02 - 0.11	92.8 - 96.2	0.11 - 0.55	3.20 - 6.11	32
ALH 84007*	20 - 500	0.10 - 0.25	< 0.02	94.1 - 96.9	0.26 - 0.35	2.64 - 4.98	52
Aubres	40 - 80	0.27 - 0.68	< 0.02	92.9 - 95.1	0.23 - 0.35	3.15 - 5.80	10
Bishopville	10 - 100	0.08 - 1.05	< 0.02	94.2 - 97.8	0.06 - 0.52	0.53 - 4.75	12
Bustee	70 - 150	0.10 - 0.46	< 0.02 - 0.07	92.1 - 93.5	0.24 - 0.33	5.11 - 6.76	8
Khor Temiki	450 - 4600	0.16 - 0.49	0.08 - 0.13	93.4 - 95.5	0.28 - 0.37	3.91 - 5.28	10
Mayo Belwa	10 - 800	0.31 - 1.37	< 0.02 - 0.25	88.2 - 95.6	0.09 - 0.65	3.53 - 11.09	29
Norton County	10 - 15000	< 0.02 - 1.31	< 0.02 - 0.69	91.5 - 96.5	0.03 - 0.52	3.08 - 7.66	62

* Includes ALH 840xx (see Table 1).

also higher variation in Ni contents. This variability is also paralleled by P and Si compositional ranges, except in Bishopville (variable Co *vs.* constant P).

The most characteristic chemical feature of aubritic metal is the relatively high concentration of Si that it has in solid solution. Figure 5 shows the Ni and Si compositional variation in eight of the aubrites studied in this work. Although the range of Si contents is large from particle to particle (from below detection limit to almost 1.4 wt.% in Mayo Belwa and Norton County), the maximum Si concentrations are, to my knowledge, unique among known compositions of metallic fractions of differentiated stone meteorites. Microprobe point analyses revealed that silicon is completely homogenized within single kamacite particles, suggesting that equilibrium in individual particles has been reached in all cases. In addition to this, there is no apparent correlation between the composition and the grain size (fig. 6), thus confirming Wasson and Wai's (1970) results.

In contrast to observations in kamacite, the distribution of silicon in taenite reflects non-equilibrium, as evidenced by the M-shaped profiles observed in all the taenite crystals (from both nuggets and smaller metallic grains) studied in this work. Si follows the same pattern as Ni, with the typical depletion and steep enrichment at the kamacite-taenite (tetrateanite) interface, and progressive depletion from the edge of the taenite grain towards the interior, as shown in fig. 7. The serrated appearance of the compositional profile of the taenite grain from section UNM 961 shown in this figure corresponds to a complicated mineralogical structure in the interior of this octahedral grain (fig. 8). Plessite (a sub-micron intergrowth of kamacite and

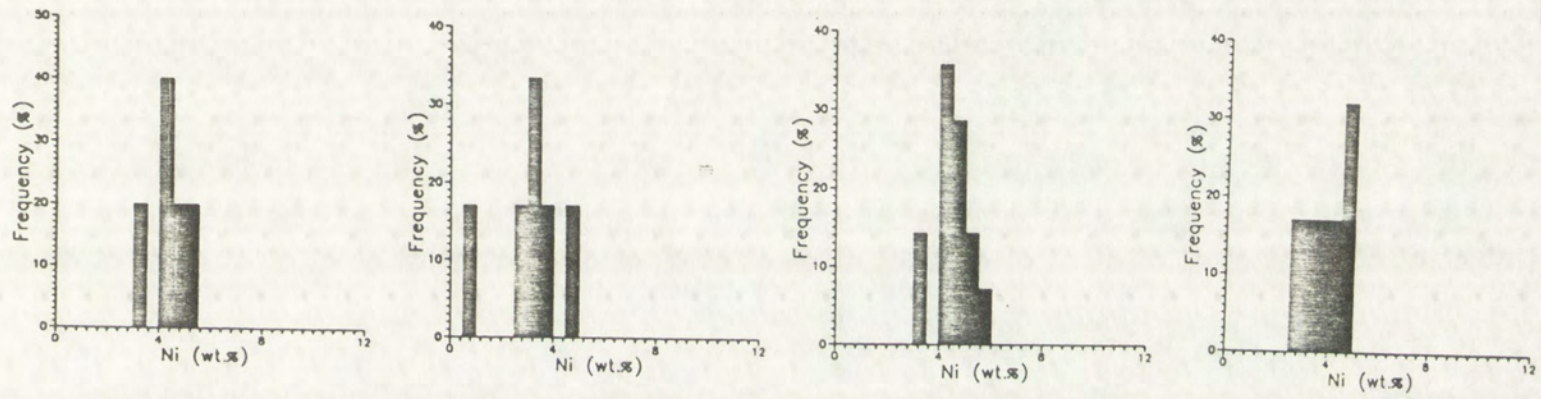

AUBRES (N=10) BISHOPVILLE (N=12) ALHA 78113 (N=32) ALH 84007* (N=52)

FIGURE 5. Distribution of Ni and Si in the metal phase of aubrites. Frequency is in % of individual analyzed grains. (N= number of grains). Figure is continued on next page.
* Includes ALH 840xx (See table 1).

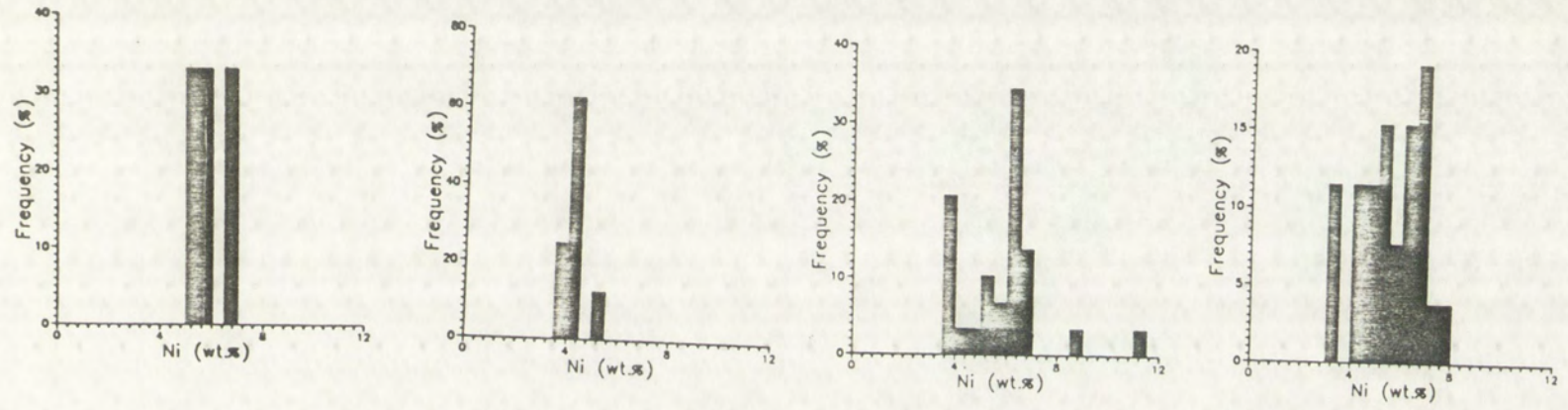

BUSTEE (N=8) KHOR TEMIKI (N=10) MAYO BELWA (N=29) NORTON COUNTY (N=62)

FIGURE 5 (cont.). Distribution of Ni and Si in the metal phase of aubrites. Frequency is in % of individual analyzed grains. (N = number of grains).

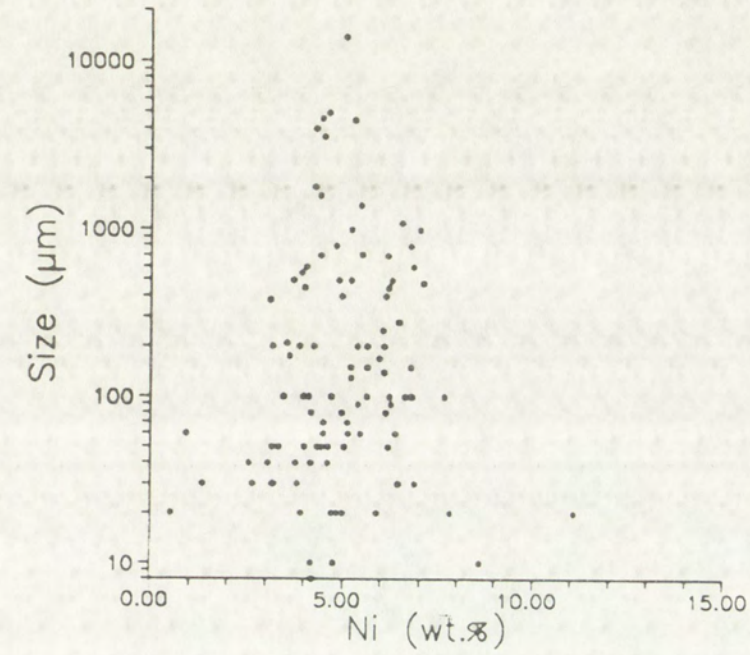

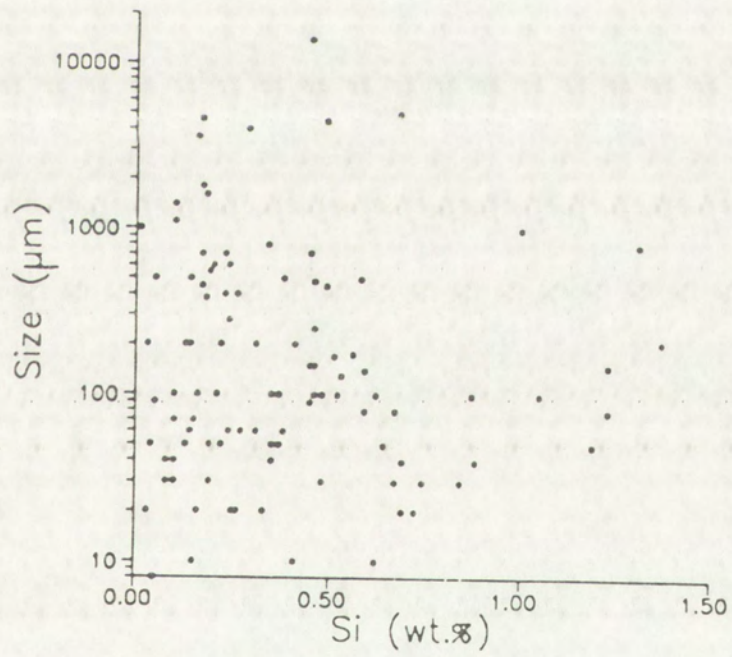

FIGURE 6.- Ni and Si variation *vs*. size in aubritic kamacite.

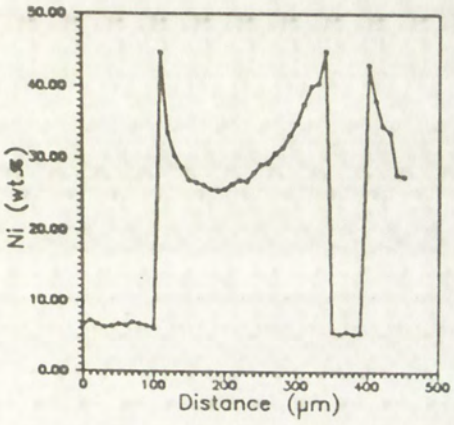

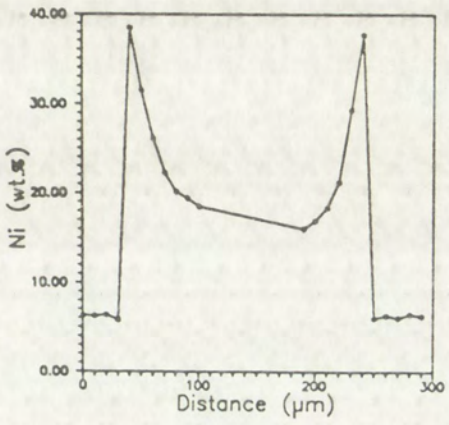

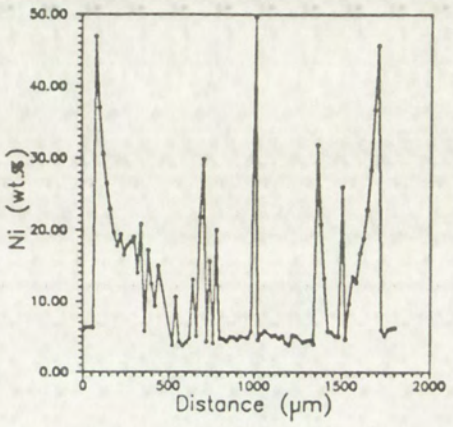

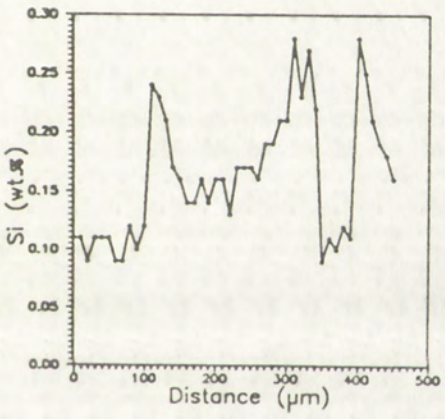

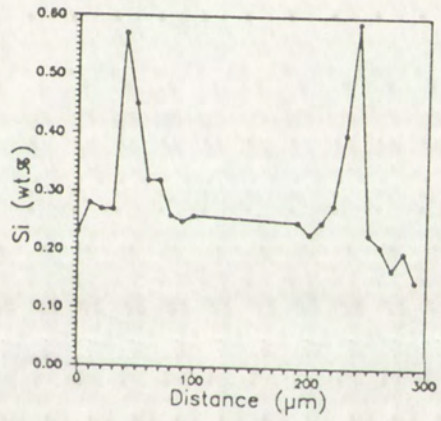

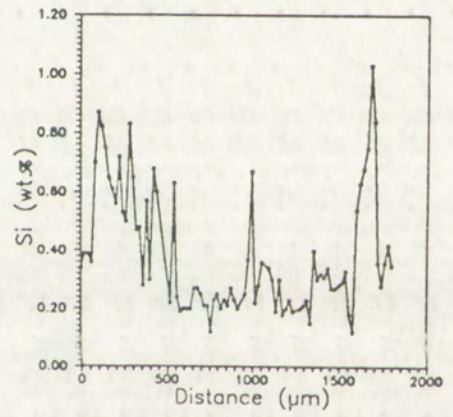

UNM 576

UNM 923

UNM 961

FIGURE 7.- Compositional profiles in taenite grains of Norton County. Notice the correlation between Ni and Si contents. Labels for each pair of diagrams indicate the thin section in which taenite grains were found.

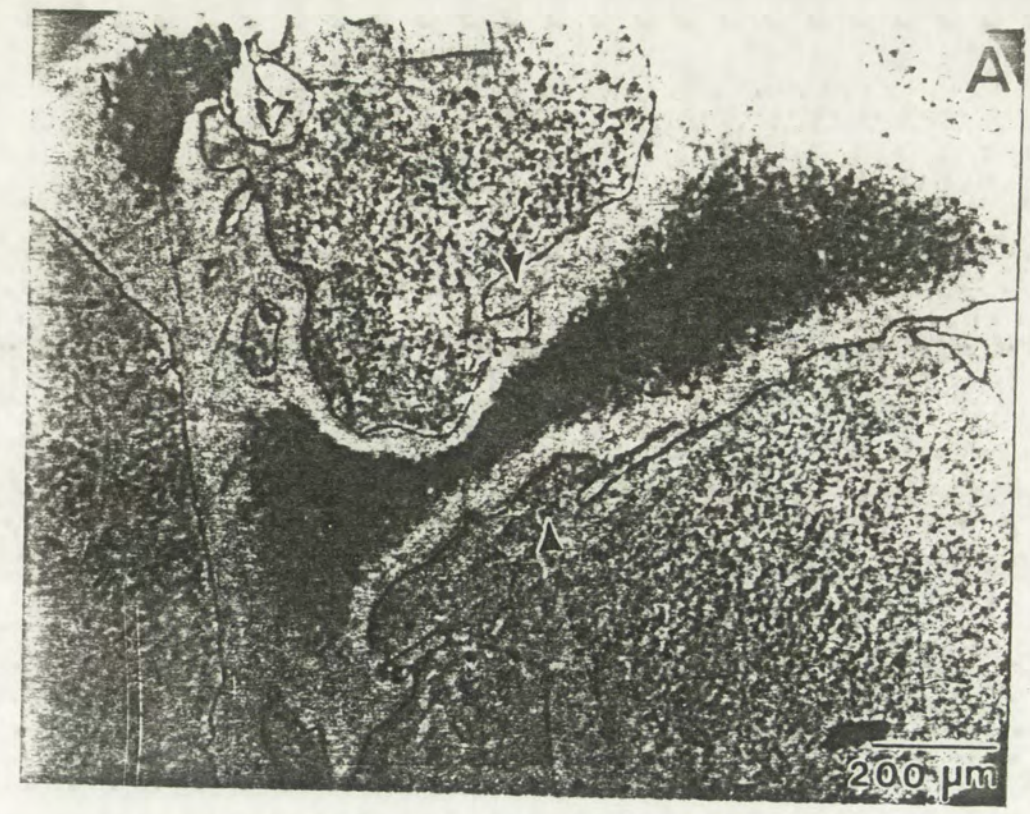

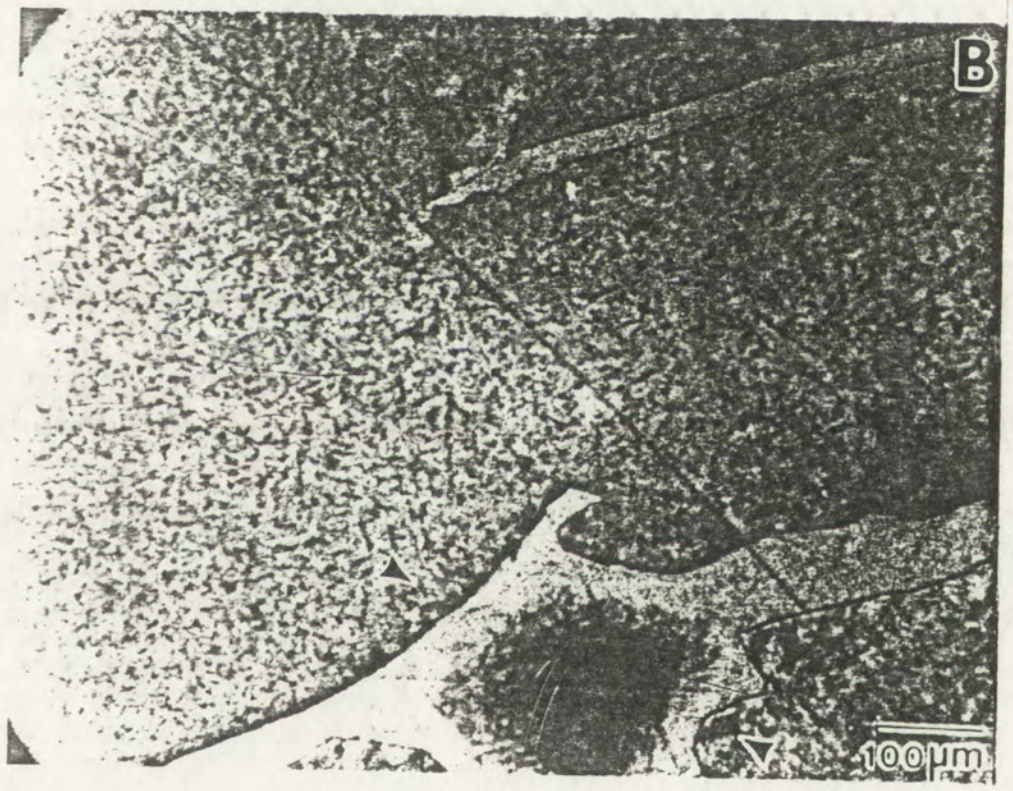

FIGURE 8.- Microphotographs of the cloudy taenite grains for which compositional profiles are given in Figure 7 (the arrows indicate the direction and length of the traverse analyses). The mottled areas in microphotographs A and B, and exsolution lamellae (C, next page) in the host kamacite are perryite.

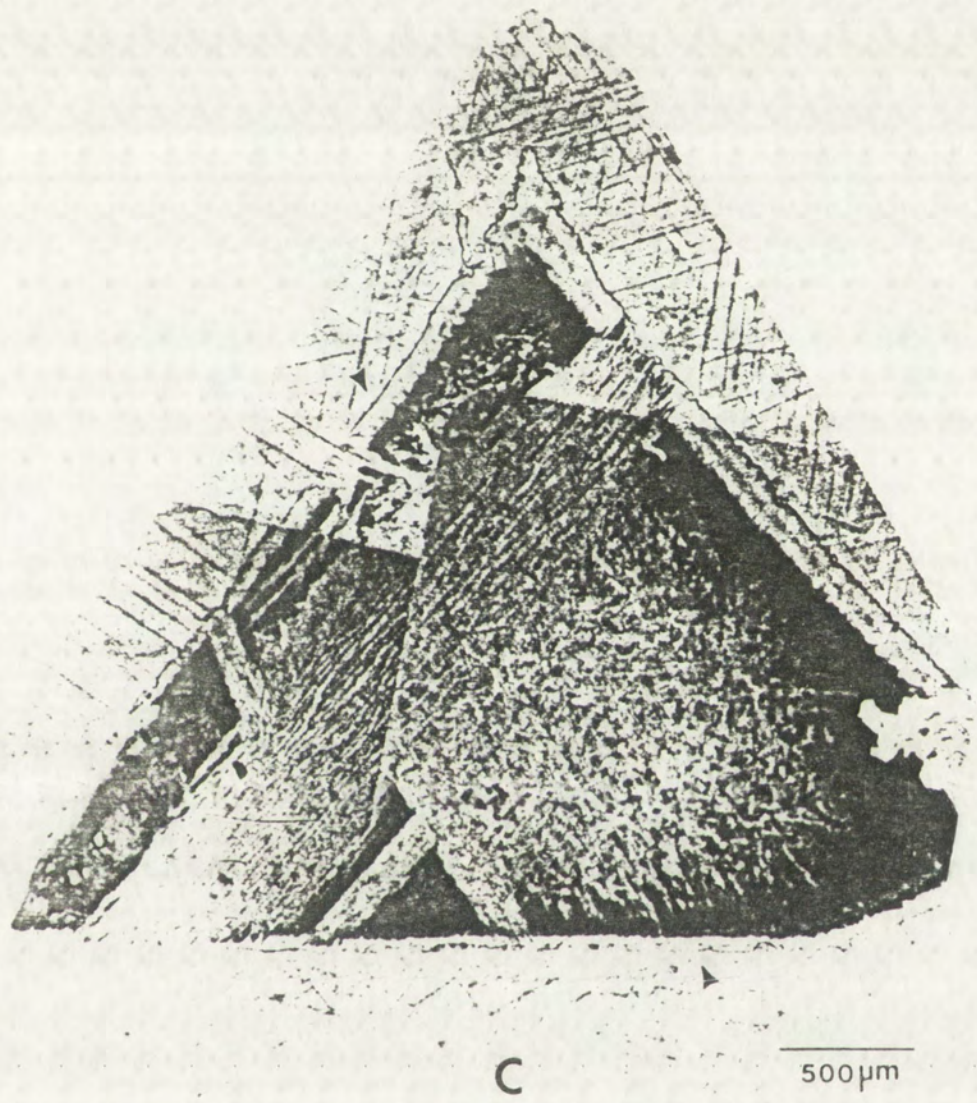

FIGURE 8. (cont.)- Microphotographs of the cloudy taenite grains for which compositional profiles are given in Figure 7 (the arrows indicate the direction and length of the traverse analyses). The mottled areas in microphotographs A and B, and exsolution lamellae (C) in the host kamacite are perryite.

taenite) occupies a large portion of this taenite crystal, thus complicating considerably the analysis of single phases. Some perryite is also present, causing the observed large enrichments in Ni and Si at approximately 750, 1000 and 1500 μm of the profile shown. On the other hand, kamacite does not display such Ni/Si correlation in any of the aubrites analyzed in this work (fig. 9).

5.1.2. Schreibersite

A summary of schreibersite compositions in aubrites is given in table 3. No significant compositional differences have been found between the rhabdite and the massive varieties.

The histograms shown in fig. 10 indicate that the distribution of compositions of schreibersite in aubrites approaches a normal Gaussian curve with a mode between approximately 35-40 wt.% Ni , but the range of compositional variation is different from meteorite to meteorite. Thus, Mayo belwa has a relatively narrow chemical variation in its schreibersites (9 wt.% Ni), whereas Norton County and ALHA 78113 show variations of approximately 20 wt.% Ni. The phosphorous content is very constant among all the analyzed schreibersites of both a single and different meteorites (14.41 wt.% in ALHA 78113 to 15.79 wt.% in Mayo Belwa).

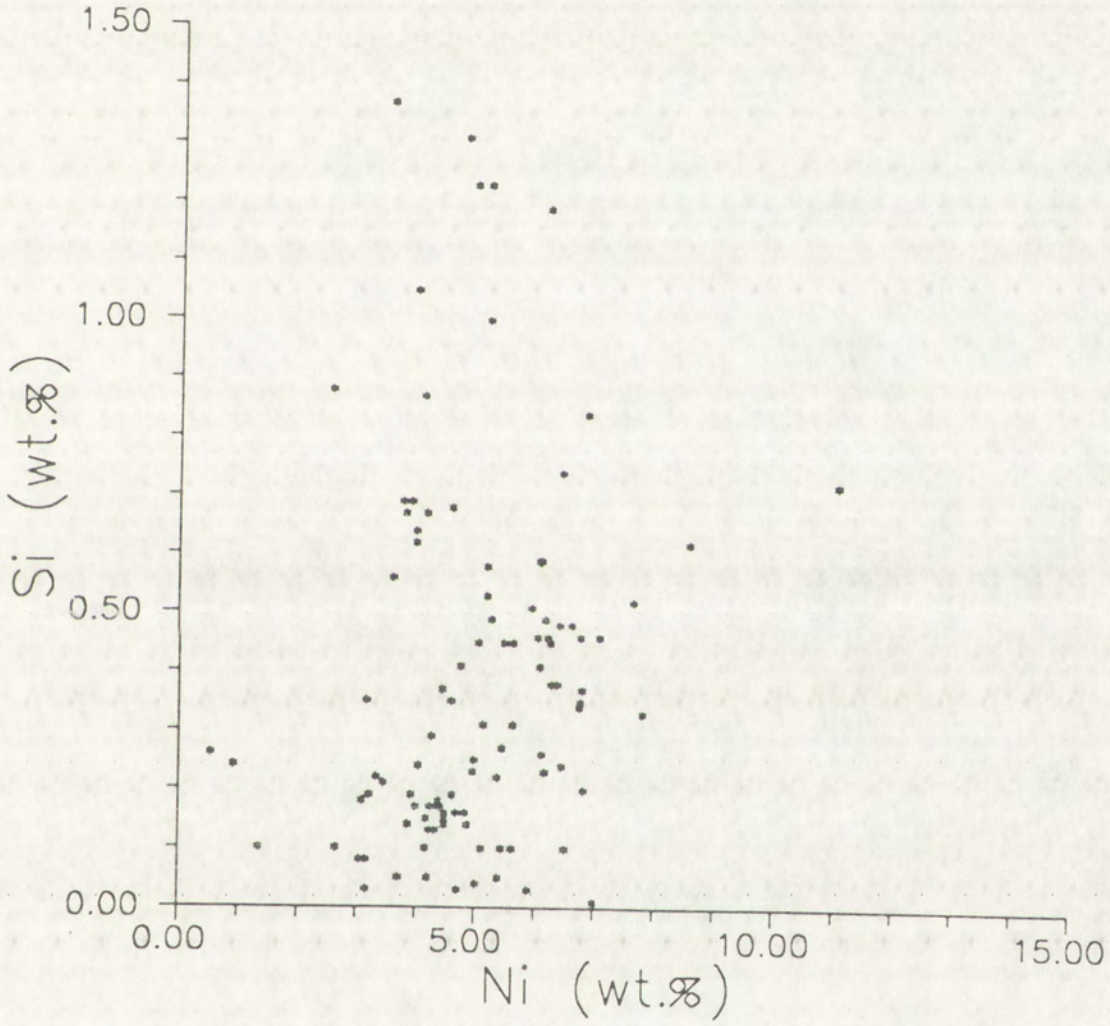

FIGURE 9.- Ni/Si variation diagram of kamacite compositions in aubrites

TABLE 3.- Compositional range of schreibersite in aubrites.

Meteorite	Size range (μm)	Si	P	Fe	Co	Ni	No. of grains
ALHA 78113	20 - 600	< 0.02 - 0.53	14.41 - 15.29	45.6 - 63.6	< 0.02 - 0.36	20.10 - 49.40	26
ALH 84007*	20 - 70	< 0.02 - 0.06	14.88 - 15.23	36.1 - 52.7	< 0.02 - 0.15	31.59 - 49.24	21
Khor Temiki	700	< 0.02	14.87	65.3	0.12	20.54	1
Mayo Belwa	10 - 60	< 0.02 - 0.32	15.00 - 15.79	67.7 - 77.1	0.03 - 0.19	6.05 - 15.15	22
Norton County	20 - 700	0.03 - 0.10	15.00 - 15.69	41.2 - 60.6	< 0.02 - 0.14	23.81 - 43.14	32

* Includes ALH 840xx (see Table 1).

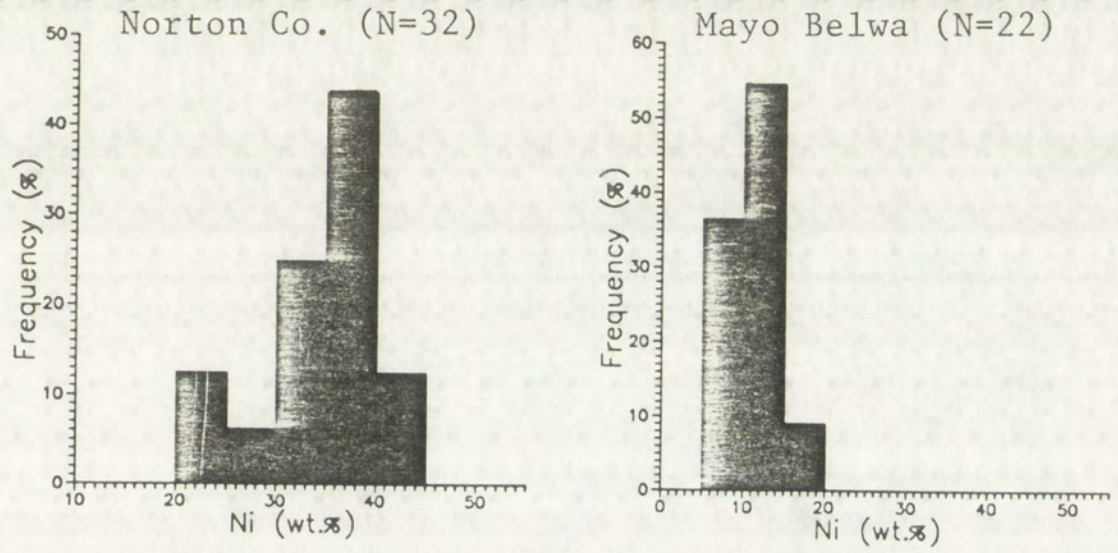

FIGURE 10.- Ni distributions in the schreibersites of Norton County, Mayo Belwa, ALHA 78113 and the totality of aubrites analyzed in this work. Frequency indicates % of individual analyzed grains. (N = number of grains).

5.1.3. Perryite

Table 4 shows a compilation of perryite compositions in Horse Creek, Mt. Egerton, and Norton County from both literaure data and this work. A detailed examination of the results listed in this table, reveals that there is a significant difference in composition between the perryites from the Mount Egerton and Norton County meteorites. Mt. Egerton perryites show Fe contents higher than Norton County's and Horse Creek's by approximately 8 wt.%. On the other hand, there is no significant compositional difference between the two varieties of perryite (lamellar and granular) of a single meteorite.

Okada *et al*. (1988) suggested the existence of two distinct populations of perryite in Norton County on the basis of their Fe contents. In this study, a quite smooth chemical variation has been observed (from 1.80 to 5.5 wt.% Fe). Okada *et al*. (1988) also suggest a direct relationship between the Si content of the kamacite host and the presence of perryite. Such correlation does not exist, since perryite has been found on kamacite grains with a wide variety of Si concentrations (for instance, in Norton County perryite-bearing metal particles have 0.45-0.60 wt.% Si, whereas other grains with concentrations of up to 1.31 wt.% Si show no evidence of exsolution of nickel silicide). I believe that the exsolution of perryite is controlled by the thermal history rather than by the composition of the kamacite host. These question will be addressed in more detail on a later section.

TABLE 4. Perryite compositions in Norton County (aubrite), Mt. Egerton (anomalous mesosiderite) and Horse Creek (hexahedrite).

Meteorite	Section	Collection	Size (μm)	Type	#	Si	P	Fe	Co	Ni	Total	Ref.
Horse Creek	-	-	-	-	-	12	5	3	-	81	101	FR65
	-	-	-	-	-	12	4	4	-	79	99	RE68
	378.1	ASU	-	-	-	12	4	(3)	-	81	100	WW70
Mt. Egerton	3272	USNM	-	-	6	11.9	3.4	(9)	-	76	100.3	WW70
	3272-1	USNM	20	Gra	10	11.97	2.91	11.03	< 0.02	74.73	100.64	
			60	Gra	21	12.30	2.44	13.02	< 0.02	72.25	100.03	
			150	Gra	33	12.23	2.70	11.98	< 0.02	73.10	100.01	
			100x10	Lam	12	12.27	2.77	12.54	< 0.02	72.35	99.93	
			200x20	Lam	25	12.26	2.68	12.62	< 0.02	71.68	99.26	
			200x20	Lam	20	12.10	2.82	13.20	< 0.02	72.11	100.23	
Norton County	170	UCLA	-	-	25	10.3	5.2	(3)	-	82	100.5	WW70
	-	-	-	-	-	10.8-11.7	4.19-4.34	1.76-1.96	n.d.	82.4-83.6	-	OK88
	-	-	-	-	-	10.1-11.6	3.37-5.02	3.20-4.73	n.d.	80.2-81.7	-	OK88
	576	UNM	30	Gra	11	11.51	4.19	3.88	< 0.02	80.01	99.59	
			40	Gra	13	10.77	4.03	1.80	< 0.02	82.55	99.15	
			60x20	Lam	5	11.00	4.11	3.07	< 0.02	81.32	99.50	
			1000x30	Lam	19	10.81	4.13	4.56	< 0.02	79.18	98.68	
	961	UNM	20	Gra	8	11.26*	3.67	6.51*	< 0.02	77.63	99.07	
			50	Gra	21	10.73	4.01	5.50	< 0.02	80.62	100.86	
			80	Gra	39	10.52	4.51	4.41	< 0.02	79.55	98.99	
			200x20	Lam	10	10.87	4.21	4.00	< 0.02	80.09	99.17	
			1000x20	Lam	25	10.72	4.35	3.87	< 0.02	79.71	98.65	

ASU - Arizona State University, USNM - U.S. National Museum, UCLA - University of California Los Angeles, Gra - granular, Lam - lamellar, # - number of analyses, FR65 - Fredriksson and Henderson (1965), RE68 - Reed (1968), WW70 - Wasson and Wai (1970), OK88 - Okada et al. (1988). Values in parentheses are calculated. Compositions marked with an asterisk are doubtful of being contaminated by kamacite.

5.2. Trace elements

I have used instrumental neutron activation analysis techniques to determine the concentrations of Ni, Co, Cr, Ir, Au, W, Ga, As, Sb and Re in 12 metal nodules from Norton County (8), ALH 84007 (1), ALH 84008 (3), and two from Mt. Egerton (Table 5). The Ni concentrations obtained on the same samples by microprobe techniques agree within the precision of the microprobe analysis. The results for Cr, W, As, Au, Ga, Ir, Re and Sb are plotted against Ni in fig. 11, together with available literature data for metal in Mayo Belwa, Mt. Egerton and Horse Creek (Wolf *et al.*, 1983), and the CI ratio line.

As discussed above, microprobe analyses show that there are no significant differences between the major and minor element compositions of a wide variety of sizes of metal particles. Accepting this, no substantial difference in trace element contents can be assumed for the fine and coarse grained populations of metal. Therefore, the trace element compositions of the analyzed metal nodules can be considered representative of aubritic metal compositions, to a first approximation. Nevertheless, given the little amount of the total metal content that these nodules represent, magnetic separation and analysis of the fine-grained fraction would be desirable in order to fully check this hypothesis.

TABLE 5.- Siderophile element contents in aubrite metal nodules.

Meteorite	Sample	Weight (mg)	Ni	Co	Cr	Ir	Au	Ga	W	Sb	As	Re
Norton County	NCL1003	84	6.28	3,585	22.0	1.2	1.0	28.0	0.4	0.6	12.3	n.d.
	NC15000	306	7.05	2,989	25.0	1.8	1.4	37.8	0.4	0.4	14.0	0.07
	NC15001	144	7.12	3,646	26.3	1.0	1.3	51.5	0.4	0.6	13.5	0.10
	NC15802	102	6.66	3,724	23.5	2.3	1.1	26.6	0.6	0.5	12.6	n.d.
	NC15804	277	7.29	3,406	6.8	2.7	1.4	41.6	0.5	0.8	16.5	0.07
	NC15810	154	6.49	3,378	15.8	2.6	1.1	34.3	0.5	0.6	12.8	0.15
	NC15833	196	7.03	3,339	n.d.	4.1	1.3	47.2	0.5	0.7	14.9	0.08
	NC15839	108	7.62	3,845	12.7	1.0	1.4	54.7	n.d.	0.8	15.1	0.02
ALH 84007	,75	10	14.78	3,128	13.3	2.1	1.6	43.1	0.8	0.6	19.5	n.d.
ALH 84008	,67	41	11.62	3,215	16.3	3.3	1.8	53.4	0.7	0.5	21.4	n.d.
	,68	233	11.51	3,412	15.8	3.1	1.2	55.1	0.6	0.7	20.0	0.09
	,70	209	8.45	3,067	14.9	2.6	1.1	48.5	0.7	0.9	18.5	0.04
Mt. Egerton	A	177	9.89	3,910	15.0	1.5	1.5	30.6	0.4	0.8	17.8	0.16
	B	192	9.68	3,888	15.7	1.9	1.5	32.26	0.4	0.6	15.4	0.11
	2626*		4.86			2.4	1.3			0.3		0.18
Mayo Belwa	1976, M.11*	48	5.80			4.0	0.6			0.5		0.34
Horse Creek	2308*	80	5.19			2.3	1.1			0.4		0.24

Values are in ppm, except for Ni (wt.%). Errors are < 5% except for Cr (10%), Sb (15%), and Re (25%). * Data from Wolf et al. (1983).

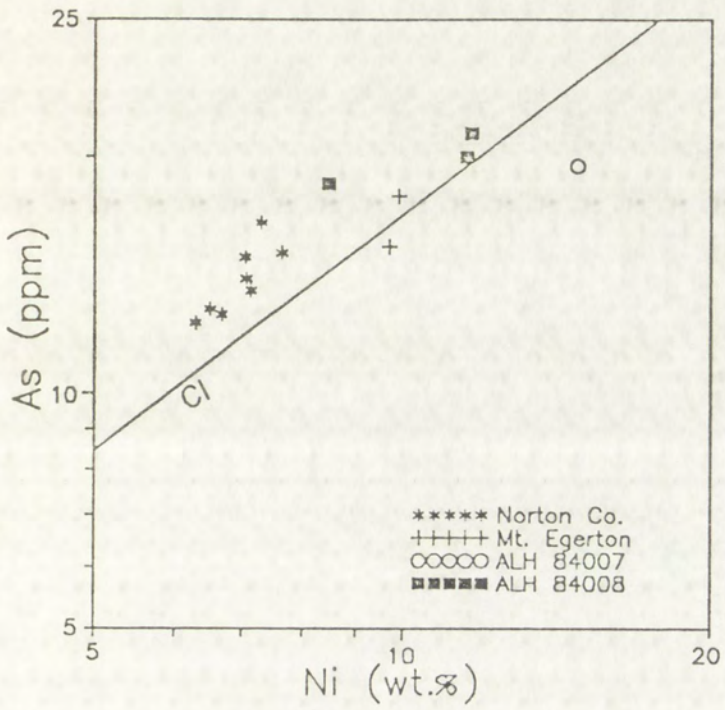

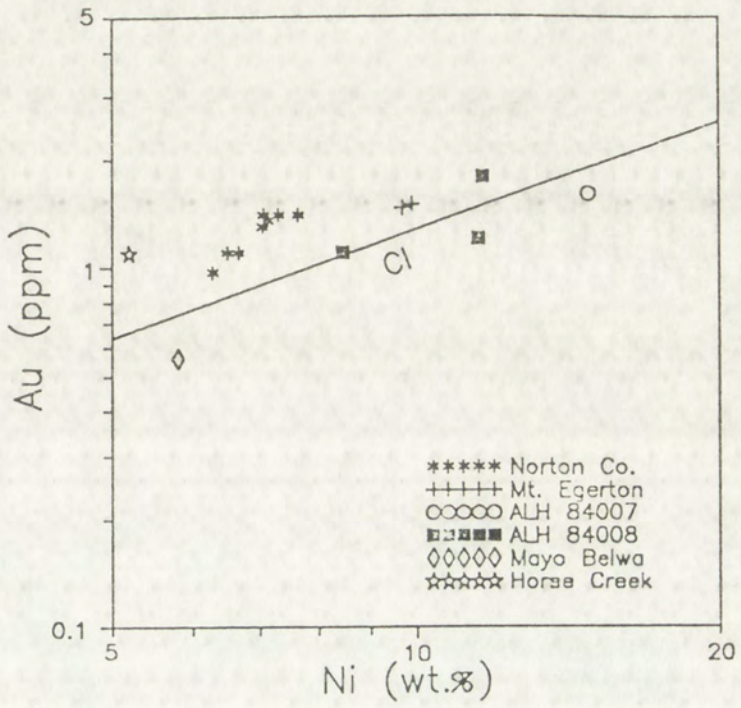

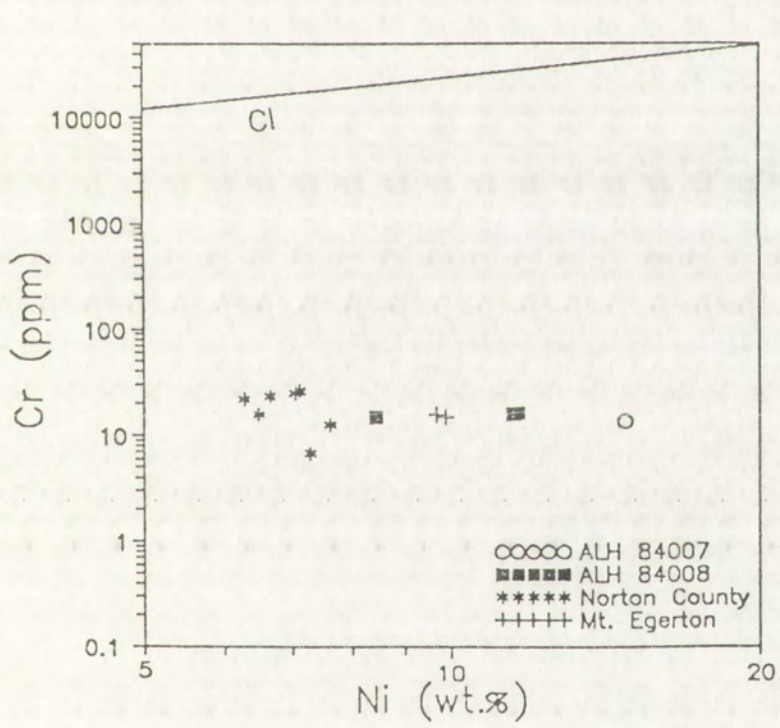

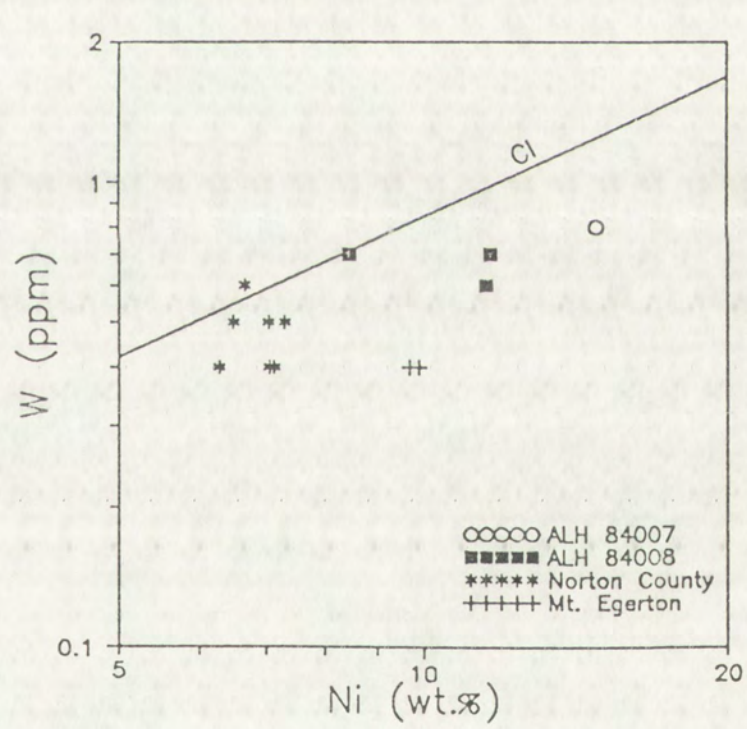

FIGURE 11.- Siderophile element vs. Ni distributions in aubrite metal nodules (including Mt. Egerton and Horse Creek). The solid line represents the CI ratio (from Anders and Grevesse, 1989). Data for Mayo Belwa and Horse Creek are from Wolf *et al.* (1983).

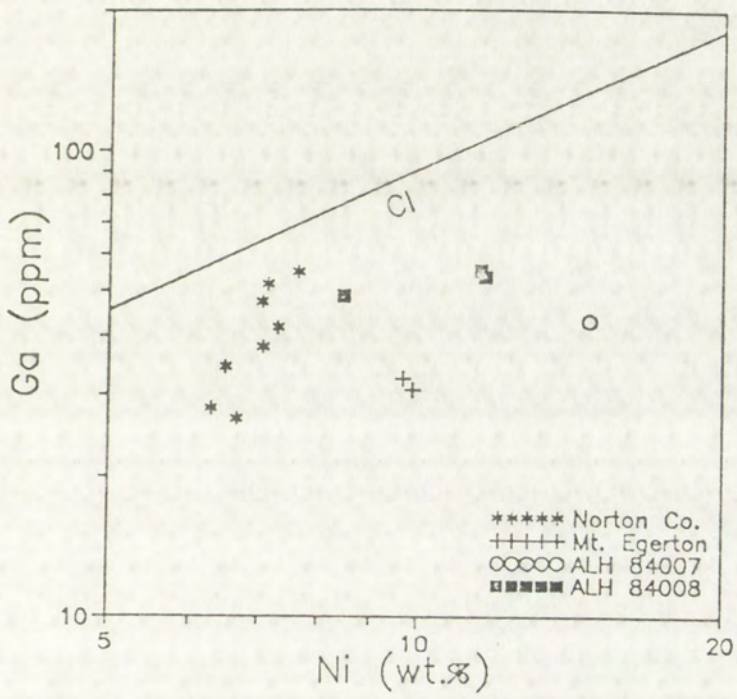

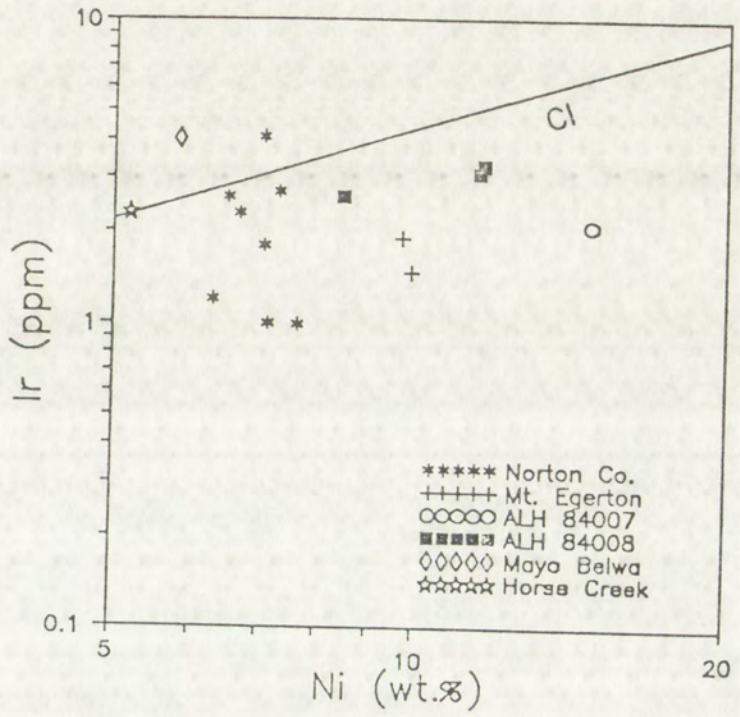

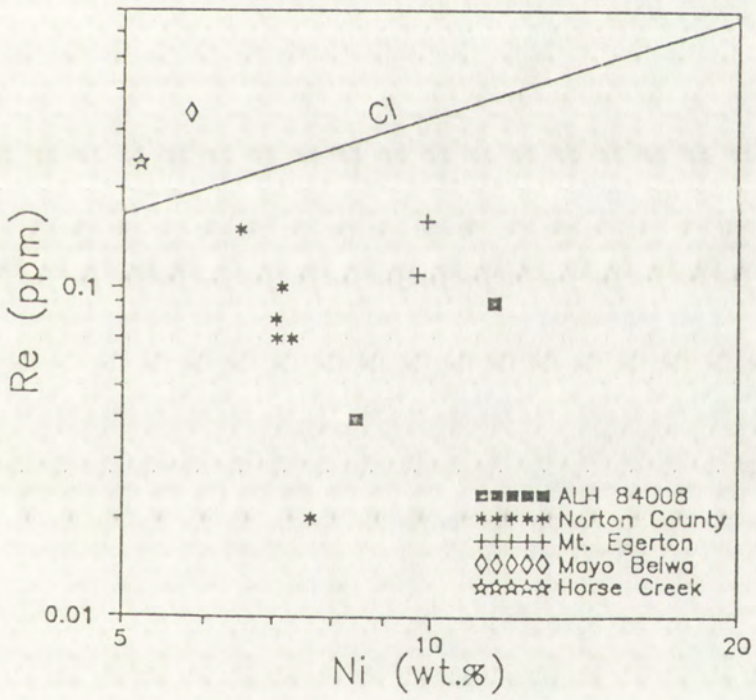

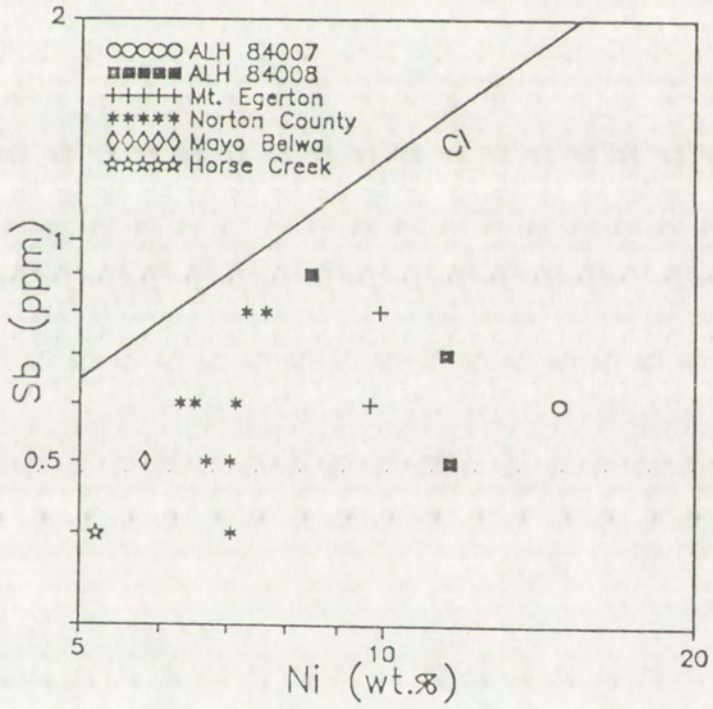

FIGURE 11. (cont.)- Siderophile element vs. Ni distributions in aubrite metal nodules (including Mt. Egerton and Horse Creek). The solid line represents the CI ratio (from Anders and Grevesse, 1989). Data for Mayo Belwa and Horse Creek are from Wolf *et al.* (1983).

The compositions of the analyzed metal particles agree with chondritic abundances (CI) within a factor of approximately 5, except for Re (one sample from Norton County is depleted approximately 10 times with respect to CI), and Cr (depletion factor is approximately 500). This evidence suggests that the trace element signature of aubritic metal is essentially chondritic, and no major fractionation processes have occurred as a result of the melting and crystallization of the metal particles studied.

The large depletion in Cr can be attributed to the concentration of this element in sulfide phases (mostly daubreelite and caswellsilverite), since no appreciable amounts of Cr exist in the silicate (Okada *et al.*, 1988). In this respect, it is important to consider the role of S in the formation of sulfides, which has been discussed in detail by Goldstein and Axon (1973) and Wai (1974). Goldstein and Axon (op.cit.) point out that S may be important in lowering the temperature of metallic melts, thereby mobilizing metal without melting silicates. This effect, however, would only extend down to temperatures in the range of 1000 C. At lower temperatures, material of Fe-FeS eutectic composition becomes enclosed in solidifying metal, and the solubility of S in the metallic phases becomes negligibly small. Sulfur is then removed from the metal by this process, becoming isolated in complex sulfide nodules (El Goresy, 1965). This a plausible mechanism to form the sulfide nodules and inclusions found in aubrites and therefore produce the observed depletion of Cr in the metal, and supports the idea of an extensive igneous history of the aubrite parent body.

6. THERMAL HISTORY

6.1. Cooling rates

Okada *et al.* (1988) determined apparent cooling rates of taenite grains in the brecciated matrix and a pyroxenitic clast of Norton County. These apparent cooling rates are in very good agreement with the ones estimated in this work from analyses of metal particles in three different aubrites (Norton County, ALH 84007 and ALHA 78113; Fig. 12). These authors estimated that the cooling rates for the analyzed aubritic metal were on the order of 5-50 deg/Ma, thus implying a long cooling history for the aubrite parent body. The existence of coarse diopside exsolution lamellae in enstatite also supports the idea of a slow subsolidus cooling. However, Okada *et al.* (*op. cit.*) considered the calculated cooling rates as a low estimate (i.e., they could be faster) by assuming that the presence of a few tenths of a percent of Si in solid solution in the metal may have a similar effect to that of P.

The presence of phosphorous increases growth rates of kamacite, causing measured cooling rates to be a factor of 3-6 too slow for a 91.9 wt.% Fe - 8.0 wt.% Ni - 0.05 wt.% P alloy (like in the Bristol, IVA iron meteorite; Saikumar and Goldstein, 1988). This composition is considered here due to its similarity to that of aubritic metal. The work by Keil *et al.* (1989) addressed the problem of the behavior of Si and P in Fe,Ni alloys, with the aim of better understanding the effect of Si in the metallographic cooling rate estimates of the metallic phases present in the Shallowater aubrite. They found that the

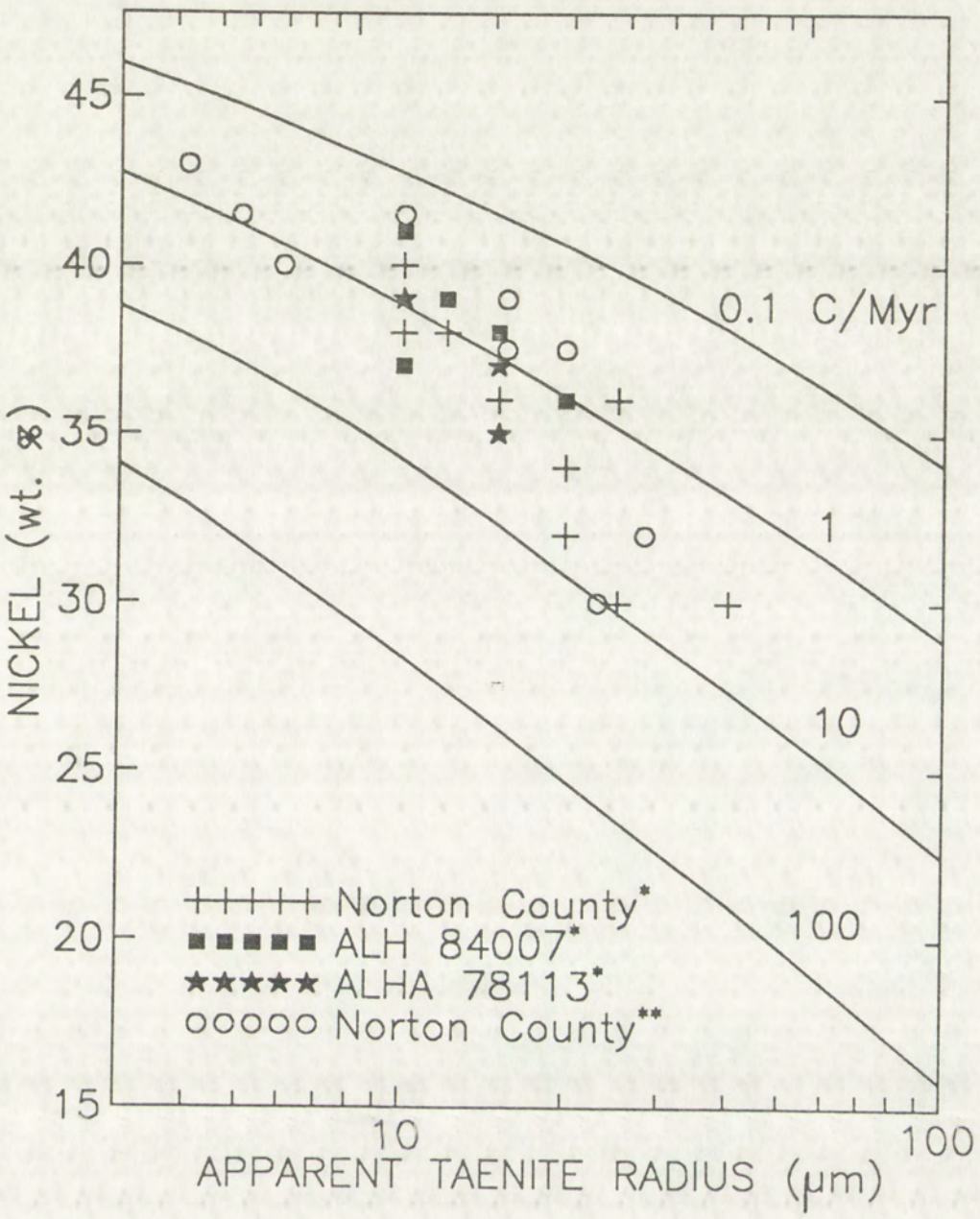

FIGURE 12.- Plot of central Ni contents of taenite grains as a function of apparent distance to the nearest edge for metal particles of Norton County, ALH 84007 and ALHA 78113. Cooling rate curves are from Willis and Goldstein (1981) for a bulk Ni content of 10 wt.%. Results from Okada *et al.* (1988) are also plotted for comparison. (*) - This work; (**) - Okada *et al.* (1988).

addition of 1 wt%. Si to an 89.7 wt.% Fe - 9.2 wt.% Ni - 0.1 wt.% P alloy increases the cooling rate by a factor of approximately 2.5 (i.e., 7.5 deg/Ma for the alloy without Si, and 18.5 deg/Ma for the alloy with Si). Therefore, the actual cooling rate of aubritic metal may be estimated as follows: 1-10 deg/Ma (apparent) x 3-6 (effect of 0.05 wt.% P) x 2.5 (effect of 1 wt.% Si) = 7-150 deg/Ma. This interval is roughly three times as large as the 5-50 deg/Ma cooling rate proposed by Okada *et al*. (1988).

The 7-150 deg/Ma variation in metallographic cooling rates implies burial depths of approximately 50 km (for 7 deg/Ma) to <10 km (for 150 deg/Ma) in a parent body of 100 km in radius, at an initial temperature of 1000 C, assuming thermal conductivities like those of silicate materials (Wood, 1967). Therefore, it is possible that metal particles in aubrites equilibrated at a variety of depths (<10-50 km) in their parent body. Although this argument does not constitute by itself evidence for the hypothesis of breakup and reassembly of the aubrite parent body proposed by Okada *et al*. (1988), it offers an alternative interpretation for the apparently small range of cooling rates of aubrites when the joint effects of Si and P are considered.

6.2. The inferred significance of perryite exsolution

I have plotted the normalized compositions of perryite grains from Norton County, Mt. Egerton and Horse Creek on four isothermal sections of the sub-solidus Fe-Ni-Si phase diagram (Fig. 13). Several interpretations can be inferred from the detailed examination of these plots:

(1) The similarity of perryite compositions between Norton County (aubrite) and Horse Creek (hexahedrite) is evident. Compositions plot coherently near or on the Ni_3Si vertex of the Ni_5Si_2-Ni_3Si-γ three-phase triangle, with one exception ("Fe-poor" perryite).

(2) The perryites from Norton County (except the Fe-poor perryite) and Horse Creek probably exsolved at a temperature between 450 and 600 C, as suggested by their proximity to the Ni_3Si vertex of the indicated three-phase triangles at those temperatures. However, Mt. Egerton perryites probably exsolved at a lower temperature, close to 450 C, and the Fe-poor perryite of Norton County is likely to represent a higher temperature (about 1000 C) exsolution product.

(3) The departure from the Ni_5Si_2 vertex of the three-phase triangle displayed by some of the Mt. Egerton perryites (Fig. 13) might represent a solid solution effect (i.e. variable contents of Ni_5Si_2 and Ni_3Si). In this case, the observed trend may be due to the presence of a Ni-rich component (Ni_xSi_y, with $x/y > 5/2$) in solid solution with Ni_5Si_2.

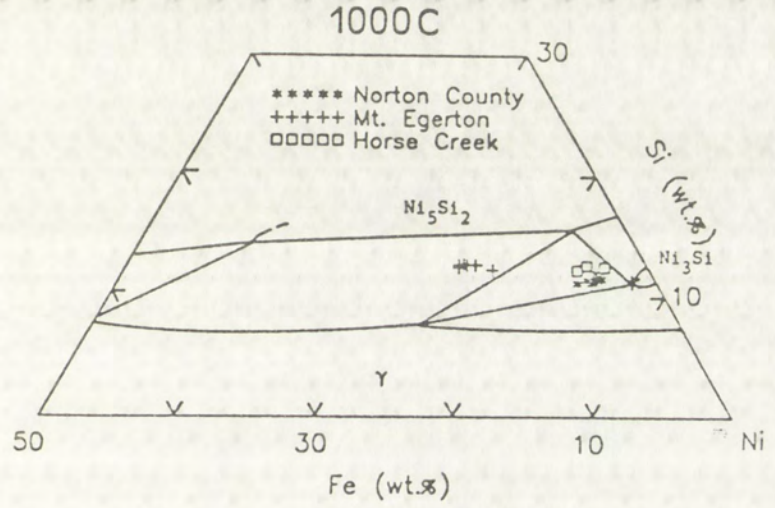

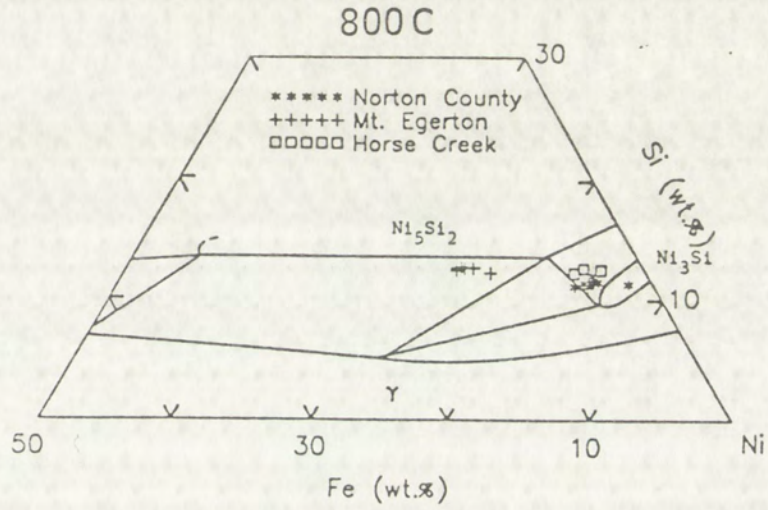

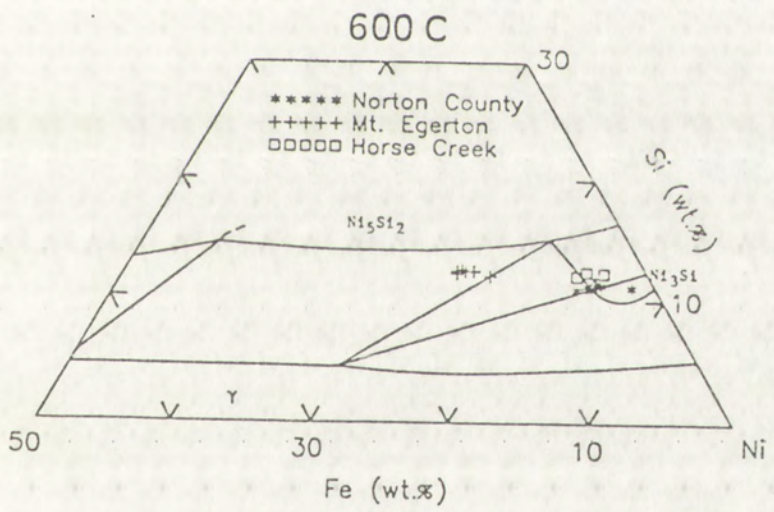

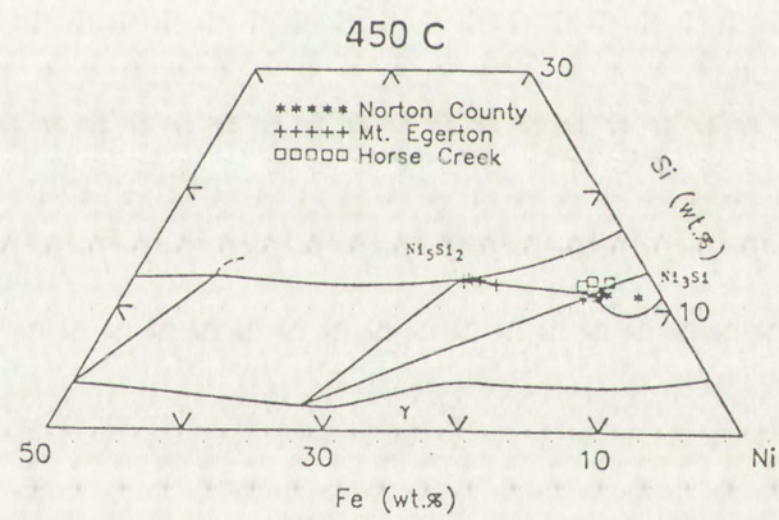

FIGURE 13.- Normalized perryite compositions of Norton County, Mt. Egerton and Horse Creek plotted on partial isothermal sections of the Fe-Ni-Si system. Phase boundary curves are from Raynor and Rivlin (1985).

The differences in mineral chemistry between Mt. Egerton and Norton County-Horse Creek perryites are probably due to differences in bulk compositions (Fe/Ni ratios) of the material from which they exsolved. The results listed in Table 6 show that the average bulk Fe/Ni ratio of perryite-bearing metal nodules in Mt. Egerton is almost a factor of two higher than that of Norton County. This might suggest that Mt. Egerton and Norton County come from different parent bodies and, following the same line of reasoning, that Horse Creek may belong to the same parent body from which Norton County was derived.

On the other hand, the existence of Fe-poor and Fe-rich perryites in Norton County might be indicative of existence of materials that equilibrated at different temperatures (between approximately 450 and 1000 C, as suggested by the plots in Fig. 13), and were subsequently mixed together in the Norton County breccia. This would require substantial differences in cooling rates for metal nodules with Fe-poor and Fe-rich perryites. As discussed earlier, the actual cooling rates for Norton County metal nodules may vary significantly from one metal particle to another. This is, in principle, consistent with the different equilibration temperatures suggested by perryite compositions. However, no cooling rate can be calculated for the nodule in which the Fe-poor perryites were found (due to the absence of taenite), and therefore, this possibility cannot be fully checked at the present stage of this work.

The most important limitation to the understanding and interpretation of perryite compositions using the proposed approach arises from the lack of

TABLE 6.- Compositions of kamacite and perryite in, and bulk analyses of perryite-bearing metal nodules in Norton County (N=5) and Mt. Egerton (N=2).

	Si	P	Fe	Co	Ni	Fe/Ni
Kamacite						
Norton County	0.28	<0.02	95.7	0.41	4.4	21.9
Mt. Egerton	1.48	<0.02	96.7	0.49	3.1	31.1
Perryite						
Norton County	10.9	4.1	3.9	<0.02	80.1	0.05
Mt. Egerton	12.2	2.7	12.4	<0.02	72.7	0.17
Bulk analyses						
Norton County	0.50	0.40	91.7	0.33	7.0	13.1
Mt. Egerton	1.87	0.10	93.7	0.28	3.7	25.3

information about the effect of a few weight percent P in the Fe-Ni-Si sub-solidus phase diagram (perryites in Horse Creek, Mt. Egerton and Norton County contain 2.4-5 wt.% P). To my knowledge, the Fe-Ni-Si-P quaternary system has not been studied yet and, until some information on this complex phase diagram is available, the interpretations given above can only be considered as a promising approximation to the significance of perryite exsolution in the thermal history of aubritic metal.

7. ORIGIN OF METAL IN AUBRITES

7.1. Clues from the depletion of siderophile elements in aubritic silicates

Equilibrium between silicates and metallic Fe,Ni reached upon melting causes a characteristic depletion in the siderophile element contents of the silicates (increasing depletion with increasing siderophile behavior). The study of such depletion can provide information about the differentiation history of the precursor material, amount of metal involved, and degree of partial melting (e.g. Newsom, 1986).

Several factors have to be taken into account in the interpretation of such abundances:

(1) The possibility that formation and segregation of an initial Fe+FeS liquid of eutectic composition took place before the completion of melting of the metal. Taylor (1989) considers this possibility unlikely but, it is important to remember that aubrites contain the greatest concentrations of sulfur of any achondrite group (Gibson et al., 1985), and it should be kept in mind that relatively high sulfur fugacities can change significantly the partitioning behavior of siderophile elements (e.g., Jones and Drake, 1983).

(2) The calculated siderophile depletions in the silicates depend on the degree of partial melting considered. This is due to the fact that

compatible and incompatible siderophile elements behave differently when either metal/liquid silicate or metal/bulk silicate (bulk = liquid + solid) distribution coefficients are taken. In this work, the influence of the melt fraction has been considered by using solid silicate/liquid silicate distribution coefficients given by Jones and Drake (1986).

(3) Metal/bulk silicate distribution coefficients are a function of temperature, composition and oxygen fugacity. The available experimental data extend only to values of log fO_2 of approximately -15 and up to 1600 C for silicate of basaltic compositions. Aubrites may have formed under significantly lower oxygen fugacity conditions (e.g., Foget *et al.*, 1989, estimated log fO_2 < -19.9 for enstatite chondrite metamorphism conditions), and their silicate composition is more ultramafic than that of basalts. These factors may have played a relatively important role in the distribution of siderophile elements between the metal and the silicate in aubrites.

(4) If substantial differences in trace element contents exist between the two textural types of metal (fine and coarse), their contribution to the observed siderophile depletion in the silicates may be completely different and would need evaluation. However, as stated before, the similarity in major and minor element composition between the fine and coarse-grained metal fractions makes this possibility unlikely.

The depletion of siderophile elements relative to the assumed initial chondritic composition is measured by comparing the abundance ratio of a siderophile in the aubrite sample to the same abundance ratio in chondritic material. The basic equation for the weight fraction of metal (X) required to achieve a certain depletion (a) in a single partial melting event has been derived by Rammensee and Wanke (1977). Assuming equilibrium between the metal and the silicates,

$$X = \frac{a - 1}{\frac{1}{D^{s/m}} + a - 1} \qquad [1]$$

where $D^{s/m}$ is the bulk metal/silicate partition coefficient for a certain element, defined as $D^{s/m} = C_i^{silicate} / C_i^{metal}$ (C_i is the concentration of the element of interest); *a* is the depletion factor relative to CI chondrites, defined as $a = [(C_i / C_{ref})_{CI}] / [(C_i / C_{ref})_{sample}]$, where C_{ref} is the concentration of a reference element for which $D^{s/m}$ is essentially zero).

Rammensee and Wanke (1977) and Palme and Rammensee (1981) have assumed equilibrium in a system containing only solid metal and liquid silicate. Newsom and Drake (1982) have shown that the ratio of silicate melt to silicate solid may have a large influence on $D^{s/m}$.

$D^{s/m}$ can be calculated from the relationship

$$D^{s/m} = \frac{F_{liq} + \frac{C^{sol}}{C^{liq}} \cdot (1 - F_{liq})}{D^{el}} \qquad [2]$$

where D^{el} is the solid-metal/silicate melt partition coefficient, F_{liq} is the fraction of silicate melt divided by the total fraction of silicates, and C^{sol}/C^{liq} is the solid-silicate/silicate-melt partition coefficient.

I have tried to overcome the paucity in experimental data for metal/silicate partition coefficients under highly reducing conditions by calculating the apparent $D^{s/m}$ from analytical data of the metal and silicate fractions of the Mt. Egerton meteorite (Wolf *et al.*, 1983). The use of this procedure is, in principle, justified by the igneous, unbrecciated nature of Mt. Egerton, and its similarity in composition to aubrites (highly reduced silicates, Si in solid solution in the metal, Watters and Prinz, 1979; identical oxygen isotope signature, Mayeda and Clayton, 1980). The apparent distribution coefficients calculated from Mt. Egerton data have been compared with experimental data for Re, Ir, Au, Ni and Ag silicate/metal partitioning provided by Jones and Drake (1986). The comparison between both sets of data (calculated and experimental) is given in Table 7.

The calculated silicate/metal partition coefficients for the considered elements are in good agreement (within an order of magnitude) with Jones and Drake's (1986) experimental data, except for Ag (the relatively chalcophile behavior of this element is a plausible reason for the observed discrepancy).

TABLE 7.- Calculated and experimental liquid-silicate/liquid-metal partition coefficients for Ni, Au, Re, Ir and Ag. Solid-silicate/liquid-silicate partition coefficients given by Jones and Drake (1986) have been used for the recalculation of $D^{s/m}$ at different degrees of partial melting.

Element	Liquid-silicate/liquid- metal partition coefficient .				
	Apparent*	Recalculated			Experimental**
		$F_{liq}=0.1$	$F_{liq}=0.5$	$F_{liq}=0.9$	
Ni	1.8×10^{-3}	2.0×10^{-4}	3.3×10^{-4}	9.5×10^{-4}	2×10^{-4}
Au	1.5×10^{-3}	same	same	same	1×10^{-4}
Re	2.9×10^{-4}	same	same	same	5×10^{-4}
Ir	2.9×10^{-4}	6.5×10^{-6}	1.2×10^{-5}	5.0×10^{-5}	5×10^{-5}
Ag	6.15	13.4	8.8	6.5	1×10^{-2}

* - From Mt. Egerton data (Wolf et al., 1983)
** - Jones and Drake (1986)

Therefore, only Ni, Au, Re and Ir have been considered in the subsequent calculations carried out in this work.

The depletion factor (Δ) is equal to $1/a$ (Eqn. 1). Therefore, rearranging Eqn. 1 we have that

$$\Delta = \frac{1 - X}{\frac{X}{D^{s/m}} - X + 1} \qquad [3]$$

Substituting the value for $D^{s/m}$ (Eqn. 2) into Eqn. [3]

$$\Delta = \frac{1 - X}{\frac{X \cdot D^{el}}{F_{liq} + \frac{C^{sol}}{C^{liq}} \cdot (1-F_{liq})} - X + 1} \qquad [4]$$

This expression allows the calculation of the expected depletion factor in the silicates for the considered elements as a function of the amount of metal (X=mass fraction of metal) and the degree of partial melting (F_{liq}= melt fraction). The calculated values of Δ are listed in Table 8, and compared (for different degrees of partial melting and amounts of metal) with abundances of these elements in the silicate fraction of aubrites (data from Wolf *et al.*, 1983) in Figs. 14, 15 and 16. From the examination of these plots, it is evident that

TABLE 8.- Calculated depletion factors for Ni, Au, Re and Ir for 10%, 50% and 90% partial melting, and 5%, 10%, 25% and 50% metal in the precursor material.

Element	Depletion factor											
	F_{liq}=0.1				F_{liq}=0.5				F_{liq}=0.9			
	X=0.05	X=0.10	X=0.25	X=0.50	X=0.05	X=0.10	X=0.25	X=0.50	X=0.05	X=0.10	X=0.25	X=0.50
Ni	4×10^{-3}	2×10^{-3}	6×10^{-4}	2×10^{-4}	6×10^{-3}	3×10^{-3}	1×10^{-3}	3×10^{-4}	2×10^{-2}	9×10^{-3}	3×10^{-3}	1×10^{-4}
Au	3×10^{-2}	1×10^{-2}	5×10^{-3}	2×10^{-3}	SAME				SAME			
Re	6×10^{-3}	3×10^{-3}	9×10^{-4}	3×10^{-4}	SAME				SAME			
Ir	1×10^{-4}	6×10^{-5}	2×10^{-5}	7×10^{-6}	2×10^{-4}	1×10^{-4}	3×10^{-5}	1×10^{-5}	9×10^{-4}	5×10^{-4}	2×10^{-4}	5×10^{-5}

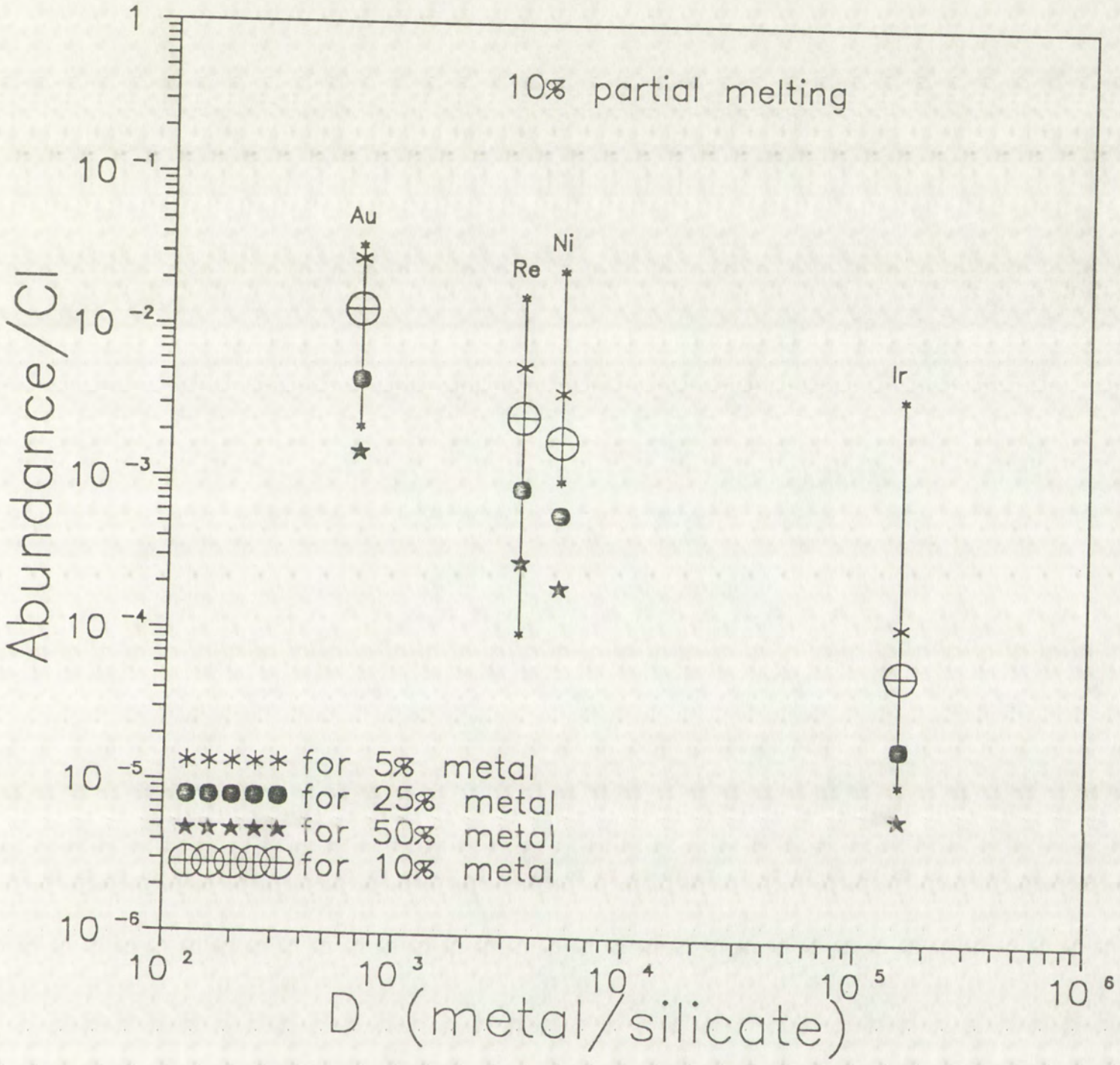

FIGURE 14.- Calculated siderophile element depletion in aubritic silicates as a function of increasing siderophile behavior. Vertical bars represent ranges in analytical data from Wolf *et al.*, 1983). Values for distribution coefficients are calculated from data for Mt. Egerton (see text for explanation). Calculated depletions in this plot are for $F_{liq} = 0.1$.

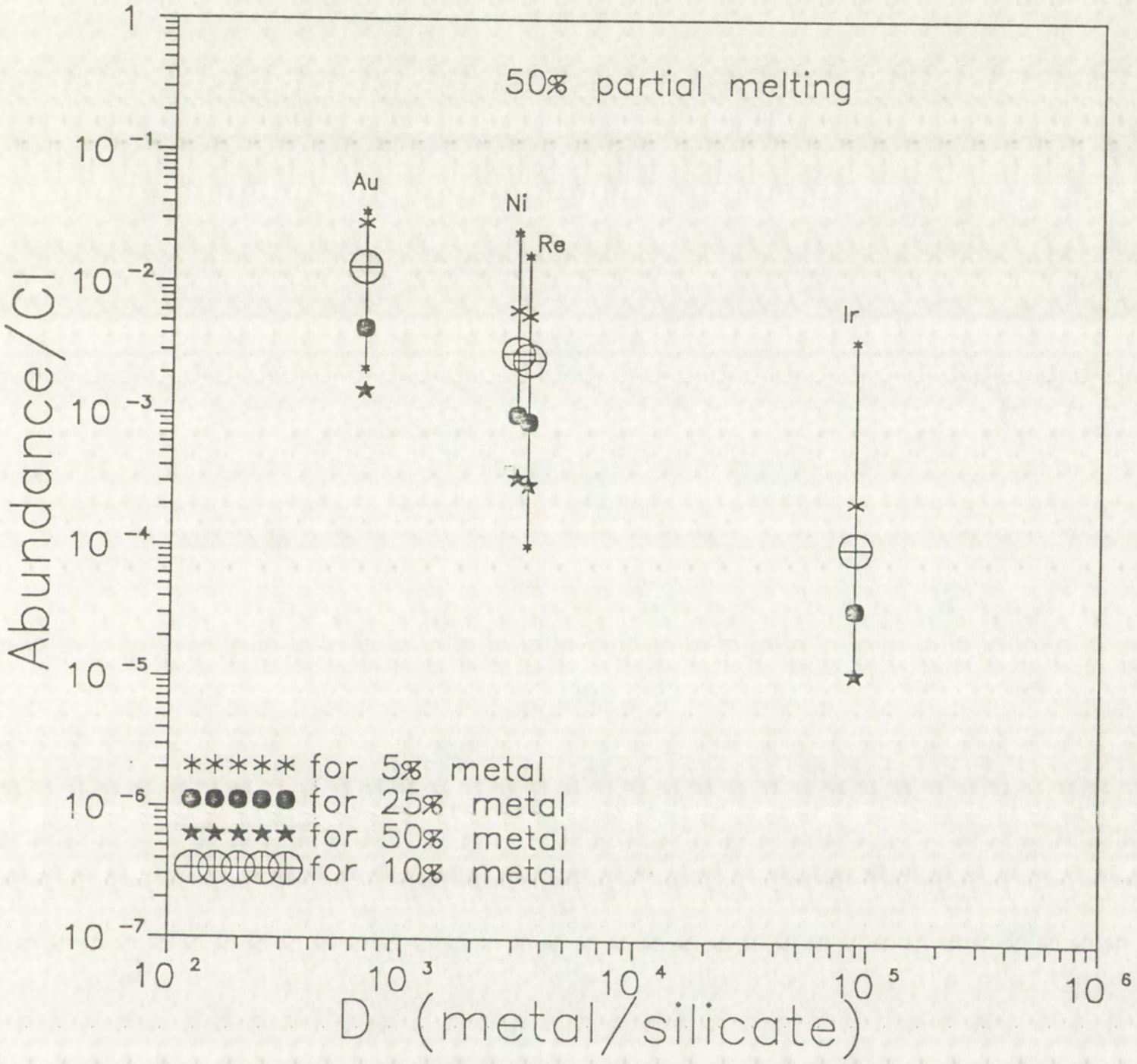

FIGURE 15.- Calculated siderophile element depletion in aubritic silicates as a function of increasing siderophile behavior. Vertical bars represent ranges in analytical data from Wolf *et al*., 1983). Values for distribution coefficients are calculated from data for Mt. Egerton (see text for explanation). Calculated depletions in this plot are for $F_{liq} = 0.5$.

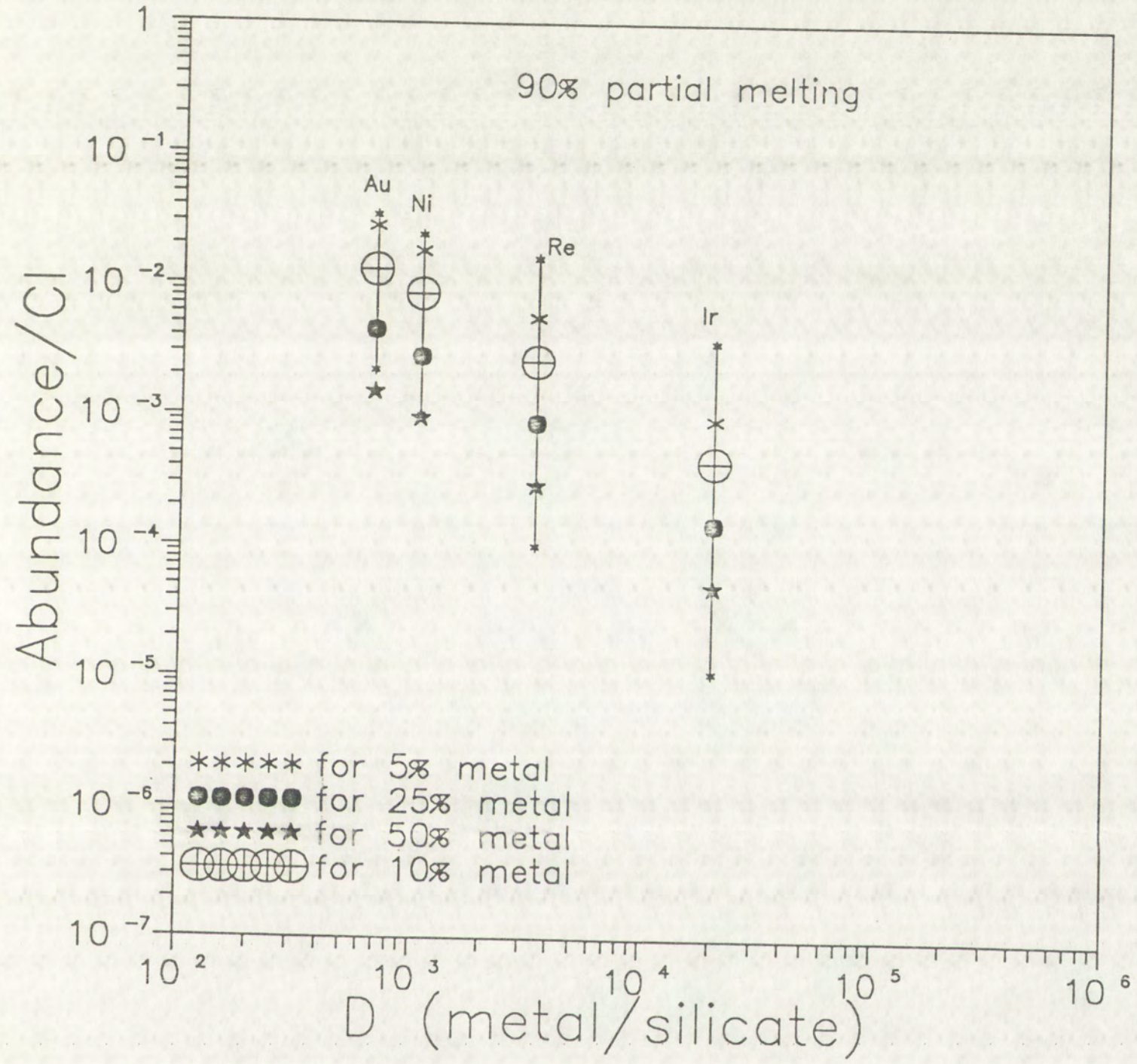

FIGURE 16.- Calculated siderophile element depletion in aubritic silicates as a function of increasing siderophile behavior. Vertical bars represent ranges in analytical data from Wolf *et al*., 1983). Values for distribution coefficients are calculated from data for Mt. Egerton (see text for explanation). Calculated depletions in this plot are for $F_{liq} = 0.9$.

higher metal/silicate partition coefficients correspond to higher depletions. This effect is indicative of metal segregation (upon melting) occurring in the aubrite parent body.

The results of these calculations show that:

(1) The amount of metal of the precursor material is the dominant factor (far more than the degree of partial melting) controlling the depletion of the siderophile elements in the silicates.

(2) The best agreement between calculated and observed depletions occurs at high degrees of partial melting (in the considered possibilities, the best agreement is found for $F_{liq}=0.90$, Fig. 16).

(3) Depletion calculations for metal fractions of 0.05 and 0.10 plot always within the observed range for aubrites (i.e., for any of the F_{liq} calculated in this work). This is not the case when higher amounts of metal (25 and 50 wt.%) are considered.

However, the large ranges in siderophile element abundances displayed by aubritic silicates do not allow an accurate specification of either the amount of metal nor the degree of partial melting involved in aubrite differentiation processes. The range of the metal amount required to produced the observed depletions in the siderophile element contents of aubritic silicates can be calculated if Eqn. [4] is rearranged in the following way (solving for X):

$$X = \frac{\Delta - 1}{\Delta - \frac{\Delta \cdot D^{el}}{F_{liq} + \frac{C^{sol}}{C^{liq}} \cdot (1-F_{liq})} - 1} \qquad [5]$$

The computed results for X, using this expression, are given in Table 9. No definitive interpretation can be given from the results listed in Table 9 on the amount of metal involved in aubrite differentiation and the degree of partial melting of the precursor material. The discrepancies between the calculated maximum and minimum amounts of metal required to produce the observed depletions might reflect (1) uncertainties in metal/silicate partition coefficients, and/or (2) a very heterogeneous distribution of the metal prior to or during the main melting episode. The large variability in Si in solid solution in aubritic metal might be indicative of local variations in oxygen fugacity (as discussed later) and, consequently, very different metal/silicate partitioning behavior for the same element may be found in a single parent body with variable local equilibrium conditions. Such an effect is likely to be responsible, at least partially, for the large variability in siderophile element contents displayed by aubritic silicates. An alternative possibility to explain such variation is that, upon melting of the aubrite precursor material, the metal segregates and concentrates heterogeneously in different parts of the parent body. As a result of this, the silicates from zones with higher amounts of metal would become depleted in siderophiles to a larger extent than those from areas with relatively less metal. The understanding of this scenario opens new questions about the efficiency of the metal segregation process in the aubrite

TABLE 9.- Amounts of metal (X) required to produce the observed depletion ranges of siderophile elements in aubritic silicates.

El.	Observed Δ		F_{liq}=0.1		F_{liq}=0.5		F_{liq}=0.9	
	Δ_{high}	Δ_{low}	X_{high}	X_{low}	X_{high}	X_{low}	X_{high}	X_{low}
Ni	$1x10^{-3}$	$2x10^{-2}$	0.17	0.01	0.25	0.01	0.49	0.04
Au	$2x10^{-3}$	$3x10^{-2}$	0.41	0.04	SAME		SAME	
Re	$1x10^{-4}$	$2x10^{-2}$	0.75	0.02	SAME		SAME	
Ir	$1x10^{-5}$	$4x10^{-2}$	0.37	0.002	0.51	0.004	0.82	0.01

parent body (i.e., the likelihood of formation of isolated metal pods as opposed to a metallic core).

7.2 Efficient vs. inefficient core formation: clues from the siderophile element contents in the metal

Several possibilities can be considered for the origin of aubritic metal: (a) in situ reduction of FeO under low oxygen fugacity conditions, in a similar way to that suggested for the origin of kamacite in the Camel Donga metal-rich eucrite (Palme *et al.*, 1988), or the formation of matrix metal in mesosiderites (Mittlefehldt, 1990), (b) extraneous (xenolithic) chondritic material, incorporated into the aubrite parent body as clasts, (c) fragments of a fractionally crystallized core from the aubrite parent body or another asteroid and, (d) disseminated globules segregated from the silicate + metal + sulfide magma (inefficient core formation).

Although enstatite meteorites formed under very low oxygen fugacity conditions, the compositions of the analyzed metal particles indicate that in situ reduction of FeO from a silicate magma is very unlikely to be responsible for their origin, since substantially lower amounts of Ni than the observed would be expected in metallic material formed in such way (*e.g.*, Palme *et al.*, 1988). In addition to this, if we assume that the parental material of aubrites was somewhat similar to enstatite chondrites, the possibility of forming

significant amounts of reduced Fe is negligible since enstatite chondrite silicates are also essentially free of iron.

Metal nodules in aubrites show well-defined igneous contacts with their silicate hosts: this strongly supports the idea that such metal is not xenolithic (chondritic) material incorporated as a result of accretionary processes or collisions between different asteroids. Chemical variations due to nebular processes have been observed in chondritic metal (e.g. Kelly and Larimer, 1977) and such variations in the material that accreted to form the aubrite parent body are certainly possible, as suggested for the origin of the metal clasts in the Bencubbin and Weatherford meteoritic breccias (Newsom and Drake, 1979). These authors based their hypothesis on the coincidence of the observed Co/Ni, P/Ni, and Ga/Ni ratios in the metal phase of these meteorites with calculated condensation curves. No such coincidence has been observed for the Co or Ga contents of the metal particles analyzed in this work; P, as mentioned earlier, is below detection in the majority of analyses, in contrast with the 0.2-0.4 wt.% P found by Newsom and Drake (op. cit.) in Bencubbin and Weatherford.

Aubrites are highly brecciated meteorites and, therefore, the possibility that their metallic fraction proceeds from a fractionally crystallized core which was mixed with mantle material as a result of impact processes must also be taken into account. However, there are two lines of evidence that make this hypothesis unlikely: (1) the siderophile element concentrations in aubritic metal found in this study indicate that its composition is roughly chondritic, except for Cr (Table 5, Fig. 10). Fractional crystallization of a metallic magma

would induce large variations in the concentrations of certain siderophiles. For instance, the Ir/Ni ratios in the so-called "magmatic" iron meteorites (believed to be fragments of fractionally crystallized asteroidal metallic cores; Wasson, 1985) show variations of up to 6000 times. As mentioned earlier, the aubritic metal inclusions analyzed in this work and others (e.g. Wolf *et al.*, 1983; Casanova *et al.*, 1990), show siderophile element/Ni ratios within a factor of 5 with respect to CI abundances. Therefore, the possibility that the studied metal nuggets represent fragments of a fractionally crystallized core can, in principle, be ruled out. However, this by no means implies that the aubrite parent body did not undergo a core formation process. As discussed earlier, the observed low abundance of metal and correlation of the siderophile element contents in the aubritic silicates with their increasing siderophile affinity (metal/silicate distribution coefficients) indicate that metal segregation was an extensive process in the aubrite parent body. The second line of evidence that argues against the metal particles being fragments of a fractionally crystallized core comes from the study of the Fe-Si phase diagram. Although, to my knowledge, no information is available on the Fe-Ni-Si liquidus equilibrium relationships (except for one projection of hypothetical primary surfaces; Raynor and Rivlin, 1985, and references therein), I believe that the ternary phase diagram can be approximated with the Fe-Si binary, due to the relative flatness of the T *vs.* composition curves of the known Fe-Ni and Ni-Si liquidus binary phase diagrams (e.g. Raynor and Rivlin, 1985, and references therein). Fractional crystallization of an Fe-Si alloy would produce solids progressively richer in Si, up to the Fe-Si eutectic composition (Fe_2Si, 20 wt.% Si at 1200 C; Kubaschewski, 1982). No such compositions have been found in any of the analyzed metal particles in aubrites and, therefore, it is unlikely that

fractional crystallization was a significant process in their formation, supporting the ideas conceived from the abundances of siderophile elements mentioned above.

Therefore, at the present stage of investigation it seems more likely that the observed metal nodules and particles in aubrites represent trapped fragments that were not completely segregated into a core. The calculations carried out by Taylor (1989) suggest that very high degrees of partial melting are needed to efficiently settle out metallic Fe,Ni into a core. For instance, melt fractions greater that 0.90 are required to sink metal particles of a few cm in diameter upon melting of an asteroid of 50-100 km in radius, as suggested by Okada *et al.* (1988) for the Norton County parent body based on cooling rate estimates. The physical setting of metal segregation processes undergoing in the aubrite parent body cannot be constrained solely by chemical data. We cannot exclude the possibility of formation of a core but, if this was the case, no samples of it are represented in the aubrites studied in this work.

7.3. Constraints on the environment of metal formation: clues from the distribution of silicon

The silicon contents of metal grains in aubrites are remarkably high and variable. To explain this, I have used a thermodynamic approach to study the main factor(s) that led to the observed variation of silicon contents in the metal phase of aubrites. In this section, I assess the role of oxygen fugacity and differences in temperature, and different models will be discussed with the aim to constrain ideas about the origin of aubritic metal. Such calculations suggest

that both differences in oxygen fugacity and/or temperature regime can readily produce large variations of the equilibrium amount of reduced silicon that enters the metallic phase. The influence of other variables (e.g. composition, crystallochemical control) is very difficult to evaluate theoretically, and their influence might not be negligible. I begin with an overview of the evaluation of the thermodynamic behavior of Si in metallic Fe,Ni alloys.

7.3.1. Thermodynamic behavior of Si in metallic Fe,Ni

Two studies have addressed the problem of the thermodynamic behavior of Si in metallic alloys, calculating an expression for the value of the Si activity coefficient. These are:

$$\log \gamma_{Si} = 1.322 - 6141/T \text{ (Baedecker and Wasson, 1975)} \quad [6]$$

and

$$\log \gamma_{Si} = 1.19 - 7070 / T + x_{Si}(18300/T-6.30) \text{ (Sakao and Elliot, 1975)} \quad [7]$$

These two models are compared in figure 17, showing that significant differences exist between both sets of results, especially for low concentrations of Si in the metal. In this work, I have used the expression for γ_{Si} given by Sakao and Elliot (1975), because it is the result of their experiments and takes into account the influence of composition (by including an x_{Si} term), whereas Baedecker and Wasson (1975) derived the expression from older data by Seybolt (1958) and do not

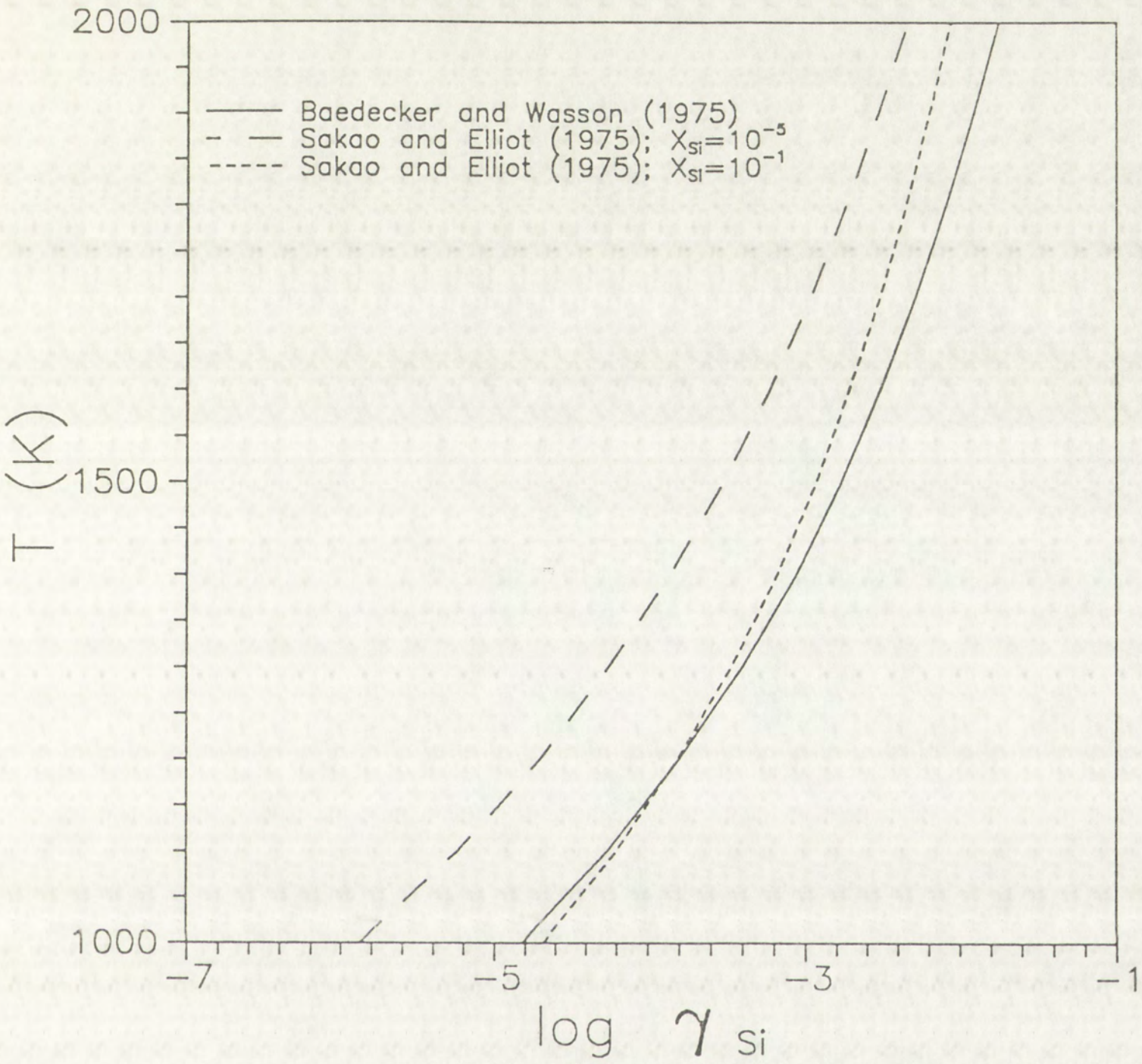

FIGURE 17.- Comparison of two different models for the activity coefficient of Si (γSi) in solid solution in metal (X_{Si} = mole fraction of Si in metal). See text for explanation.

consider the variation of the activity coefficient as a function of composition.

We can now address the question of the influence of oxygen fugacity and temperature variations on the observed metal compositions. For this, I have represented the distribution of Si between aubritic metal and silicates using the following reaction:

$$Si + Mg_2SiO_4 + O_2 = 2MgSiO_3 \qquad [R.1]$$

where Si represents the silicon in solid solution in the metal (reduced state). In the following thermodynamic study the forsterite (Mg_2SiO_4) and enstatite ($MgSiO_3$) are assumed to be pure, and oxygen is considered to behave ideally. Enstatite meteorites are one of the very few natural systems where this assumption may represent reality very closely, due to the very low iron contents that these two silicates display and the extremely low oxygen fugacities under which they formed (*e.g.* Keil, 1968, 1989; Fogel *et al.*, 1989).

7.3.2. The role of oxygen fugacity

Assuming that the phases present are pure and in equilibrium, we can use the integrated form of the Gibbs-Helmholtz equation to establish, for a certain temperature, the equilibrium concentrations of Si expected in solid solution in the metal at different values of oxygen fugacity.

The equilibrium constant for the above considered reaction can be written as

$$K = \frac{(a_{MgSiO_3})^2}{a_{Si} \cdot a_{Mg_2SiO_4} \cdot f_{O_2}} \qquad [8]$$

As noted, both enstatite and forsterite in aubrites can be considered, to a good approximation, as pure Mg-endmembers with activities equal to unity.

The activity of Si in the metallic alloy can be expressed as

$$a_{Si} = \gamma_{Si} X_{Si} \qquad [9]$$

where γ_{Si} and X_{Si} are, respectively, the activity coefficient and mole fraction of silicon in the metal. If we accept the validity of Eqn. [7] for γ_{Si} given by Sakao and Elliot (1975), we can rewrite the expression for K as

$$K = \frac{1}{\left[10^{\left(1.19 - \frac{7070}{T} + X_{Si} \cdot \left(\frac{18300}{T} - 6.3\right)\right)}\right] \cdot X_{Si} \cdot f_{O_2}} \qquad [10]$$

On the other hand, we know that at equilibrium,

$$K = \exp\left(-\frac{\Delta G^0_{rxn}}{R \cdot T}\right) \qquad [11]$$

For the considered reaction, $\Delta G^0_{rxn} = 2\,\Delta G^0\,(MgSiO_3) - \Delta G^0\,(Mg_2SiO_4)$, since $\Delta G^0\,(O_2) = 0$ and $\Delta G^0\,(Si) = 0$.

The Gibbs-Helmholtz equation can be now used to calculate the values of ΔG at different temperatures. The relationship between ΔG and T in this equation is given by

$$\left[\frac{\partial\left(\frac{\Delta G^0}{T}\right)}{\partial T}\right]_P = -\frac{\Delta H^0}{T^2} \qquad [12]$$

Assuming that the value of ΔH^0 is approximately constant in the temperature interval considered in the present calculations (1000-1600 °C), we can integrate

$$\int_{\Delta G^0_{ref}}^{\Delta G^0} d\,\frac{\Delta G^0}{T} = -\Delta H^0 \cdot \int_{T_{ref}}^{T} \frac{dT}{T} \qquad [13]$$

The temperature dependence of ΔG^0 can then be expressed as

$$\Delta G = T \cdot \left(\frac{\Delta G^0_{ref}}{T} + \Delta H^0_{ref} \cdot \left(\frac{1}{T} - \frac{1}{T_{ref}} \right) \right) \qquad [14]$$

Equating expressions [10] and [11] and substituting the derived expression for ΔG^0 we have that

$$\frac{1}{\left[10^{\left(1.19 - \frac{7070}{T} + X_{Si} \left(\frac{18300}{T} - 6.30 \right) \right)} \right] \cdot X_{Si} \cdot f_{O_2}} = \exp - \left[\frac{\frac{\Delta G^0_{rxn}(ref)}{T_{ref}} + \Delta H^0_{rxn}(ref) \cdot \left(\frac{1}{T} - \frac{1}{T_{ref}} \right)}{R} \right] \qquad [15]$$

where,

ΔG^0_{rxn} (ref) = -870.4 kJ mole^{-1}

ΔH^0_{rxn} (ref) = -925.1 kJ mole^{-1}

T_{ref} = 298.15°K (25°C)

R = 8.31441 kJ mole^{-1}°K^{-1}

The values for ΔG^0_{rxn} and ΔH^0_{rxn} have been calculated from data given by Robie *et al.* (1978).

Solving Eqn. [15] for fO_2, the equilibrium oxygen fugacity required to put a certain amount of silicon (X_{Si}) in the metal, at a certain temperature (T) can be written as:

$$f_{O_2} = \frac{\exp\left[\dfrac{\dfrac{\Delta G^0_{rxn}(ref)}{T_{ref}} + \Delta H^0_{rxn}(ref) \cdot \left(\dfrac{1}{T} - \dfrac{1}{T_{ref}}\right)}{R}\right]}{X_{Si} \cdot \left[10^{\,1.19 - \frac{7070}{T} + X_{Si} \cdot \left(\frac{18300}{T} - 6.30\right)}\right]} \qquad [16]$$

I have computed the fO_2 values that satisfy Eqn. [16], and plotted the results on a log fO_2 vs. X_{Si} diagram (Fig. 18). It can be appreciated from the study of this plot that, considering the equilibrium reaction mentioned above and at approximately the melting temperature of pure enstatite (1580 °C), it is possible to generate the whole variation in silicon contents observed in aubritic metal ($5x10^{-5} < X_{Si} < 1x10^{-2}$) by changing the oxygen fugacity approximately three log fO_2 units.

The presence of graphite in aubrites suggests that the oxygen fugacity in the system of interest can also be represented by the following reaction:

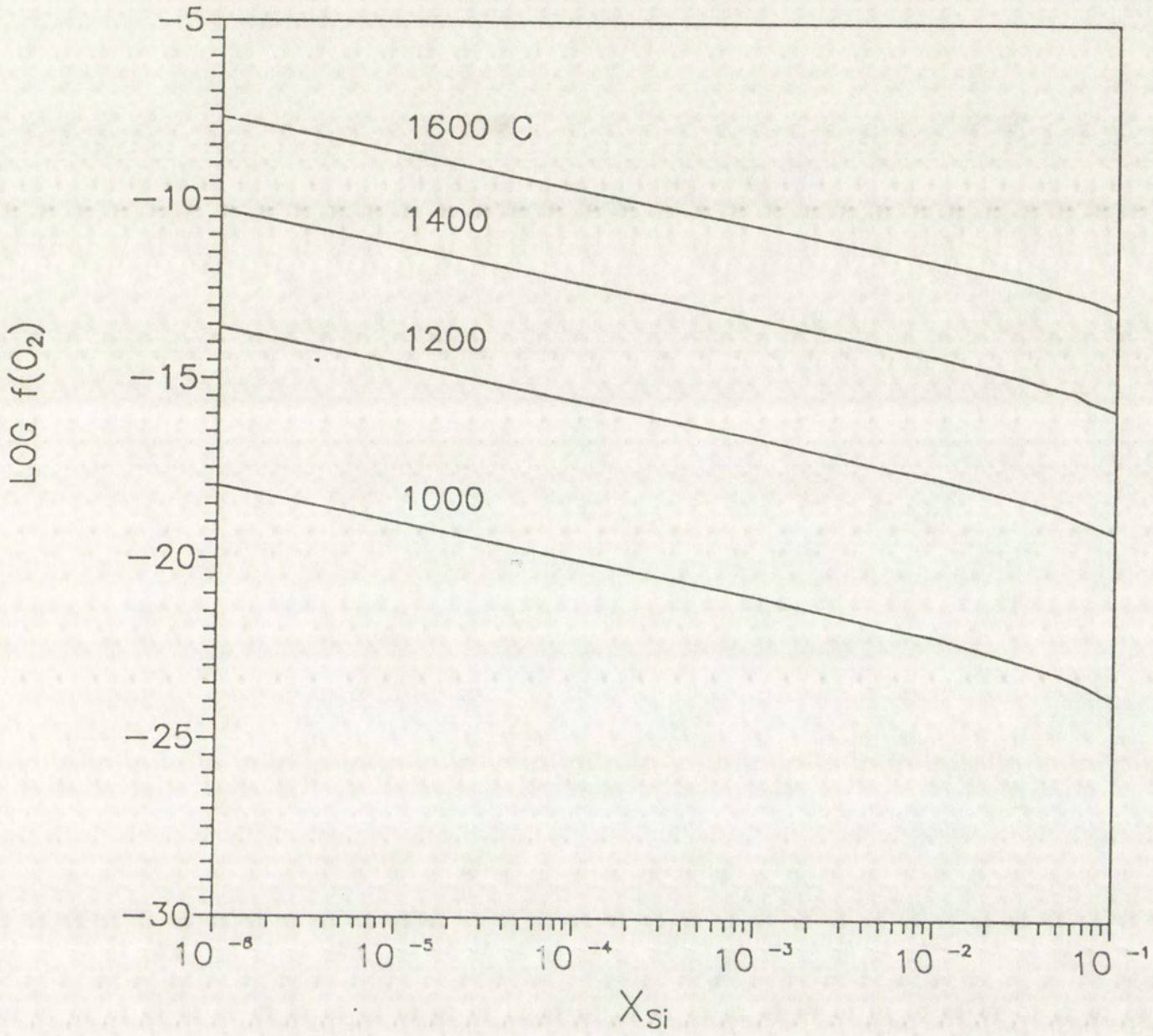

FIGURE 18.- Equilibrium silicon contents (mole fractions) expected in the metal phase as a function of oxygen fugacity, assuming non-ideal behavior of the silicon in the metal (see text for explanation).

$$C_{(s)} + 1/2\ O_{2(g)} = CO_{(g)} \qquad [R.2]$$

Assuming that graphite is a pure substance and that oxygen and carbon monoxide behave ideally, the relationship between the equilibrium constant for this reaction (K) and the partial pressures of the gases involved is

$$K = p(CO) / [p(O_2)]^{1/2} \qquad [17]$$

where *p* refers to the partial pressure of the indicated gas species.

Adding reactions R.1 and R.2 we can formulate the effect of carbon on the Si amount that enters the metal as follows:

$$2CO + 2Si + Mg_2SiO_4 = 2C + 2MgSiO_3 \qquad [R.3]$$

If the system is open with respect to CO (*e.g.* carbon monoxide is removed by outgassing), this reaction provides a viable mechanism to produce different amounts of Si in the metal (represented by the reduced Si component in the reactants). According to Le Chatelier's principle, *a reaction in equilibrium which is subject to a perturbation will tend to restore the equilibrium condition by progressing towards the side of products or reactants so that the perturbation is minimized.* Therefore, as CO escapes from the system, more reduced silicon and forsterite will be produced, and graphite and enstatite consumed. If all reduced silicon goes into the metal in solid

solution, this reaction allows the formation of Fe,Ni with different concentrations of Si, depending on the original carbon content. Assuming that we have unlimited supply of enstatite and forsterite (which is a good assumption for enstatite meteorites), the production of reduced Si in reaction R.3 will depend on (1) the efficiency of CO outgassing, (2) the initial carbon content and (3) the rate of the reaction. These are, to my knowledge, unconstrained parameters due to the lack of experimental data on this type of chemical system. Therefore, at this point no quantitative estimates can be made, but such mechanism should be considered as a viable possibility to produce the observed variation of Si contents in aubritic metal.

7.3.3. The role of temperature variations

Local differences in temperature can also play a very important role in the distribution of Si between the metal and the silicate fractions. Following a similar approach to that used in the study of the influence of oxygen fugacity, I have derived an expression which relates X_{Si} to temperature, for given values of fO_2.

Equating expressions [8] and [11], we have

$$\exp - \left(\frac{\Delta G^0_{rxn}}{R \cdot T} \right) = \frac{1}{a_{Si}} \cdot \frac{1}{f_{O_2}} \qquad [18]$$

Taking the natural logarithm of this expression,

$$\frac{-\Delta G^{0}_{rxn}}{R \cdot T} = - \ln a_{Si} - \ln f_{O_2} \qquad [19]$$

The natural representation of Sakao and Elliot's (1975) expression for the activity coefficient of Si in metal can be written as

$$\ln \gamma_{Si} = 2.303 \cdot \left(1.19 - \frac{7070}{T} - 6.30\, X_{Si} + \frac{18300}{T} \cdot X_{Si}\right) \qquad [20]$$

Substituting [20] into [19], we obtain

$$-\frac{\Delta G^{0}_{rxn}}{R \cdot T} = -2.741 + 14.51\, X_{Si} + \frac{1}{T} \cdot (16282 - 42144\, X_{Si}) - \ln X_{Si} - \ln f_{O_2} \qquad [21]$$

On the other hand, the integrated form of Gibbs-Helmholtz equation can be rewritten as

$$\frac{\Delta H^0_{ref}}{T} - \frac{\Delta G^0}{T} = \frac{\Delta H^0_{ref}}{T_{ref}} - \frac{\Delta G^0_{ref}}{T_{ref}} \qquad [22]$$

which multiplied by 1/R becomes:

$$\frac{\Delta H^0_{ref}}{R \cdot T} - \frac{\Delta G^0}{R \cdot T} = \frac{\Delta H^0_{ref}}{R \cdot T_{ref}} - \frac{\Delta G^0_{ref}}{R \cdot T_{ref}} \qquad [23]$$

Substituting the expression for $\Delta G/RT$ obtained in Eqn. [21] into Eqn. [23] we have

$$\frac{\Delta H^0_{ref}}{RT_{ref}} - \frac{\Delta G^0_{ref}}{RT_{ref}} =$$

$$= \frac{\Delta H^0_{ref}}{R \cdot T} + 14.51\ X_{Si} - 2.741 + \frac{1}{T}\ (16282 - 42144\ X_{Si}) \qquad [24]$$

$$- \ln X_{Si} \quad - \ln f_{O_2}$$

Grouping similar 1/T terms and factorizing out the T we arrive to the following equation:

$$T = \frac{\frac{\Delta H^0_{ref}}{R} - 42144\ X_{Si} + 16282}{\frac{\Delta H^0_{ref} - \Delta G^0_{ref}}{R \cdot T_{ref}} - 14.51\ X_{Si} + \ln X_{Si} + \ln f_{O_2} + 2.741} \quad [25]$$

which relates the temperature and mole fraction of silicon in the metal, at a certain value of oxygen fugacity.

The calculations carried out show that the amount of silicon that enters the metal in reduced state is strongly dependent on temperature (i.e., small variations of T induce large variations of X_{Si}). The results of these calculations are plotted in Fig. 19 showing that at the oxygen fugacities expected for aubritic metal-silicate equilibrium (log fO_2 << -11), a maximum variation of only about 200 degrees is required to produce the observed Si compositional range in the metal ($5x10^{-5} < X_{Si} < 1x10^{-2}$).

7.3.4. Discussion

If local differences in oxygen fugacity are the main factor controlling the metal-silicate equilibrium, then we can think of the following scenario: the aubrite parent body consisted originally of some kind of enstatite chondrite-like material that was initially heterogeneous with respect to the distribution and amount of carbon. Upon melting of this precursor material, a series of ultramafic magma pods may be formed; these magma bodies undergo

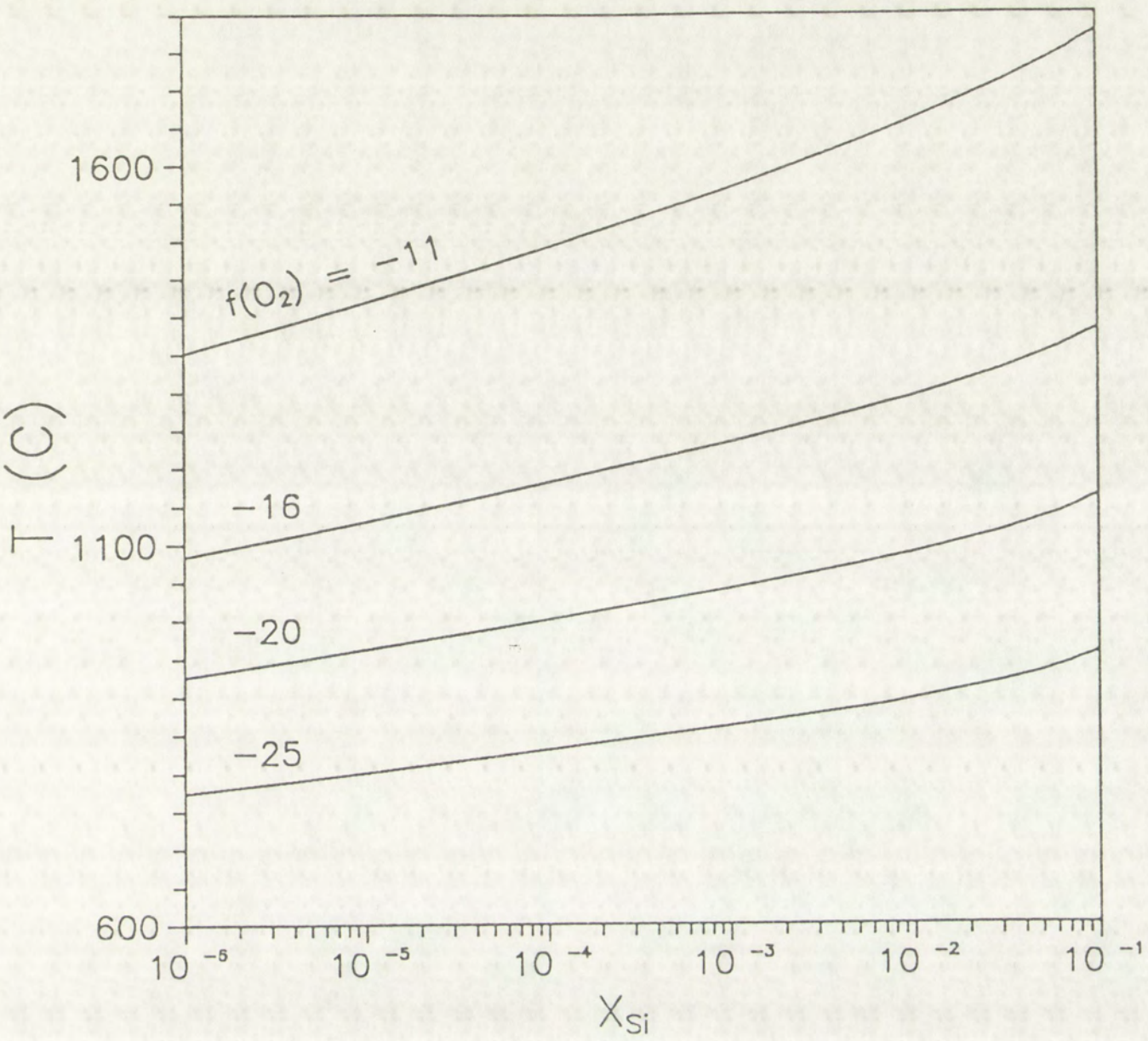

FIGURE 19.- Equilibrium silicon contents (mole fractions) expected in the metal phase as a function of temperature, assuming non-ideal behavior of the silicon in the metal (see text for explanation).

outgassing of carbon monoxide to different extents, depending on the local abundance of carbon. Crystallization in equilibrium under these conditions would then be a viable mechanism to produce the observed variations in Si concentration in the metal. Another end-member possibility can be thought of by considering multiple planetesimals which accreted under different oxidizing conditions and were then melted. However, given the large compositional variation (with respect to Si) observed in aubritic metal, the number of different planetesimals required is too large and makes this possibility unlikely.

On the other hand, if local variations in temperature in the aubrite parent body are responsible for the compositional heterogeneity of the metal, a different scenario has to be considered. A heterogeneous reheating (cooling) process is required to account for the existence of zones in the same parent body which equilibrated at different temperatures. However, it has to be kept in mind that differences from one metal particle to another in their respective closure temperatures for the diffusion of Si are also possible. This factor could also have an effect in how much silicon can enter different metal particles. Dodson's (1973) work developed a theoretical expression for T_c:

$$T_c = \frac{E_a / R}{\ln \frac{- A \cdot R \cdot T_c^2 \cdot D^0}{a^2 \cdot E_a \cdot \frac{dT}{dt}}} \qquad [26]$$

where,

E_a = activation energy

R = perfect gas constant = 8.31441 kJ $mole^{-1} \circ K^{-1}$

A = numerical constant depending on geometry (55 for a sphere, 27 for a cylinder, 8.7 for a plane)

D^0 = pre-exponential factor from Arrhenius' relation for the diffusion coefficient of an element *i* (D_i), where $D_i = D_i^0 \exp(-E_a/RT)$

a = characteristic diffusion dimension of the system

dT/dt = cooling rate

It is evident from this equation that differences in cooling rate can produce variations in closure temperature. However, at this point no quantitative evaluation of the influence of dT/dt on T_c can be carried out for the diffusion of Si in Fe,Ni alloys due to the lack of experimental data on the kinetics of such process.

It is very difficult to determine which has been the main controlling factor (*i.e.*, chemical heterogeneities or temperature regime) on producing the observed variations of Si contents in aubritic metal. Several lines of evidence (e.g. Keil, 1989; Wolf *et al.*, 1983; Wheelock *et al.*, 1989) suggest that the aubrite parent body underwent a substantial degree of partial melting. In such a physical context, it seems unlikely that convection may have homogeneized completely the molten aubritic material. This allows the possibility that several magma pods with significantly different carbon contents can be preserved, and the differences in oxidation state (local equilibrium) may subsequently have played an important role in producing the chemical heterogeneity of the metal.

8. RELATIONSHIPS WITH OTHER METEORITE GROUPS

8.1 Enstatite chondrites

It has been extensively argued that aubrites must have formed from a precursor material similar to the enstatite chondrites, but significantly different from the ones represented in meteorite collections (e.g. Keil, 1989, and references therein).

Silicon contents in the metal of enstatite meteorites display different degrees of variation. In EH chondrites, X_{Si} (mole fraction of silicon in the metal) varies between approximately $5x10^{-2}$ and $7x10^{-2}$, and for EL chondrites, $X_{Si} \simeq 2x10^{-2}$-$7x10^{-2}$ (mole fractions have been calculated from the data given by Keil, 1968); for aubrites, $X_{Si} \simeq < 5x10^{-5}$-$1x10^{-2}$. From these values, several observations can be made:

(1) The maximum concentration of Si in solid solution in the metal is approximately the same for the two groups of enstatite chondrites, and slightly lower for aubrites.

(2) An apparent paradox lies in the fact that EH chondrites which, in general, are the most unequilibrated members of the group (i.e., those that display higher variation in fayalite and ferrosilite contents of the olivines and pyroxenes, respectively), show the most equilibrated compositions with respect to Si for the metal (i.e., smaller compositional range).

(3) Aubritic metal shows a variation in silicon content significantly larger (at least three orders of magnitude) than any of the two other enstatite chondrite groups.

The calculations carried out in the course of this work suggest that heterogeneous cooling may control to some extent the distribution of Si in the metal. However, the fact that the Si contents of metal also vary significantly in the highly equilibrated ELs suggests that local equilibrium conditions are responsible for Si variations. This supports the idea that differences in fO_2, due to heterogeneities on the distribution of C in the precursor material, may be responsible for the large compositional variability found for Si in the metal of aubrites.

The siderophile element depletion calculations for the silicate fraction of aubrites do not place definitive constraints on the amount of metal involved in the igneous differentiation of the aubrite parent body. This is mainly due to the uncertainty of the metal/silicate partition coefficients under very reducing conditions. Nevertheless, the results of such calculations are suggestive of high degrees of partial melting and relatively low metal content for the precursor material from which aubrites formed (probably lower than that of known enstatite chondrites, which average 23.5 wt.% Fe,Ni for EHs, and 18.9 wt% Fe,Ni for ELs; Keil, 1968). Experimental work under highly reducing conditions is needed to verify this possibility.

8.2 Iron meteorites

The next logical problem to address regarding the possible relationships between aubritic metal and other metal-rich meteorite groups can be stated with the following question: Do we have any samples of the "missing" metal represented as iron meteorites in our collections?

The best candidate for this is, undoubtedly, Horse Creek, an anomalous hexahedrite. The relationship of this rock with enstatite meteorites was first proposed by Wasson and Wai (1970) on the basis of its high concentration of Si in solid solution in the metal and the presence of perryite. The similarity between the compositions of Horse Creek and Norton County perryites found in the present study reinforces this idea. Horse Creek could then very well be one of the metal pods which formed upon melting and inefficient core formation in the aubrite parent body.

If the high amount of silicon in metal is such a unique characteristic of enstatite meteorites, it could be used as a parameter to look for possible relationships with other irons. Wai and Wasson (1969, 1970) identified high Si concentrations in only two of nineteen iron meteorites which displayed evidence of formation under low oxygen fugacity conditions. These are Tucson and Nedagolla (ataxites with 0.8 and 0.14 wt.% Si, respectively, in the metal). However, their low Ga (Tucson: 0.94 ppm; Nedagolla: 0.65 ppm) and high Cr (Tucson: 2200 ppm; Nedagolla: 2600 ppm) concentrations are very different from those observed in aubritic metal and make the possibility of a

genetic relationship unlikely, suggesting that highly reducing conditions of formation are not exclusive to the parent bodies of enstatite meteorites.

8.3. "Anomalous" stony-irons

8.3.1. Mt. Egerton (anomalous mesosiderite)

Mt. Egerton is a highly reduced, metal-rich enstatite meteorite, very similar to aubrites due to its igneous nature and similarity in composition of the metal and silicate fractions (e.g., high Si in the metal and very low Fe in the enstatite, Watters and Prinz, 1980; oxygen isotope composition very close to those of aubrites, Mayeda and Clayton, 1980). This meteorite is, however, unbrecciated, and has little textural resemblance with enstatite achondrites. Another difference is the composition of the perryite, which in Mt. Egerton has an Fe/Ni wt%. ratio of approximately 0.15 whereas in Norton County perryite Fe/Ni = 0.02-0.07. As discussed in a previous section of this study, this difference in perryite chemistry probably denotes substantially different Fe/Ni bulk compositions of the original materials from which they formed. Subsequently, Mt. Egerton may represent yet another parent body of the enstatite meteorite clan (different parent bodies have been proposed for EH chondrites, EL chondrites, aubrites, and Shallowater; Keil, 1989, and Keil et al., 1989, and references therein).

9. CONCLUSIONS

This work provides the first systematic study of the metal phase of enstatite achondrites. The comparison between the chemical composition of aubritic metal and theoretical models developed in the course of this study proposes additional constraints on previous ideas about the magmatic and metamorphic evolution of the aubrite parent body, and opens new areas of interest in the study of the metal phase of differentiated asteroidal and planetary bodies.

The main conclusions of this study can be summarized as follows:

(1) There is a significant variation of the silicon contents of aubritic Fe,Ni. This compositional range may be due to differences in oxygen fugacity conditions, caused by local heterogeneities in the distribution of carbon in the precursor material from which aubrites formed. Differences in temperature regime (*i.e.* cooling rate) could also be responsible, at least in part, for the observed variability of Si compositions in the metal. However, quantitative estimates of the relative influence of chemical heterogeneities and/or temperature cannot be carried out until experimental data are available on the kinetics of metal-silicate reactions, and the diffusion of Si in Fe,Ni alloys.

(2) The better understanding of the significance of perryite exsolution may provide important clues about the thermal evolution of aubrites. The results obtained in this work suggest that different metal

nuggets from Norton County equilibrated at different temperatures after they crystallized. Differences in closure temperatures for the diffusion of Si into the metal (determined by variations in grain size and/or cooling rate) may, however, be an important additional parameter to take into consideration. This possibility reinforces the importance of acquisition of experimetal data on diffusion of Si in metallic alloys.

(3) Although there is evidence of metal segregation in the aubrite parent body, the metal present in known aubrites was probably never part of a fractionally crystallized core. It is more likely that the studied metal represents trapped particles that never became large enough to sink efficiently in the silicate magma.

(4) The precursor material that melted to form aubrites was probably similar to enstatite chondrites, but it might have had a significantly lower amount of metal. This interpretation is, however, strongly dependent on assumed metal/silicate partition coefficients. Consequently, at the present stage of this work this possibility has to be considered as a plausible working hypothesis, since experiments on partitioning behavior of siderophile elements under highly reducing conditions are needed to address in a more quantitative manner the problem of the metal content of the aubrite precursor material.

(5) Mt. Egerton, an anomalous mesosiderite related to the aubrites, probably comes from yet another enstatite meteorite asteroid. With this, the number of parent bodies of the enstatite meteorite clan

would be extended to five: EH, EL, aubrites, Shallowater and Mt. Egerton. On the other hand, Horse Creek, an anomalous hexahedrite, may come from the aubrite parent body, as suggested by its compositional and mineralogical similarity with aubritic metal. It may thus represent the biggest known sample of the above mentioned disseminated metal globules which formed as a result the inefficient settling of metal into a core.

10. REFERENCES

Anders E. and Grevesse N. (1989) Abundances of the elements: meteoritic and solar. *Geochim. Cosmochim. Acta*, **53**, 197-214.

Baedecker P.A. and Wasson J.T. (1975) Elemental fractionations among enstatite chondrites. *Geochim. Cosmochim. Acta*, **39**, 735-765.

Biswas S., Walsh T., Bart G. and Lipschutz M.E. (1980) Thermal metamorphism of primitive meteorites - XI. The enstatite meteorites: origin and evolution of a parent body. *Geochim. Cosmochim. Acta*, **44**, 2097-2109.

Brett R. and Keil K. (1987) Enstatite chondrites and enstatite achondrites (aubrites) were not derived from the same parent body. *Earth Planet. Sci. Lett.*, **81**, 1-6.

Buchwald V.F. (1969) Iron meteorites: tables relating the Widmanstatten angles to the plane of section. *Geochim. Cosmochim. Acta*, **33**, 152-153.

Buchwald V.F. (1975) Handbook of Iron Meteorites, 3 vol. University of California Press, 1418 pp.

Casanova I., Newsom H.E., Scott E.R.D. and Keil K. (1990) Origin of metal in aubrites: siderophile element abundances in cm-sized metal nodules of Norton County. *Lunar Planet. Sci.*, **XXI**, 172-173.

Dodson M.H. (1973) Closure temperature in cooling geochronological and petrological systems. *Contrib. Mineral. Petrol.*, **40**, 259-274.

Drake M.J., Newsom H.E. and Capobianco C.J. (1989) V, Cr and Mn in the Earth, Moon, EPB, and SPB and the origin of the Moon: experimental studies. *Geochim. Cosmochim. Acta*, **53**, 2101-2111.

Easton A.J. (1986) Studies of kamacite, perryite and schreibersite in E-chondrites and aubrites. *Meteoritics*, **21**, 79-93.

El Goresy A. (1965) Mineralbestand und Strukturen der Graphit- und Sulfideinschlusse in Eisenmeteoriten. *Geochim. Cosmochim. Acta*, **29**, 1131-1151.

Floss C., Strait M.M. and Crozaz G. (1990) REE and the petrogenesis of the aubrites. *Geochim. Cosmochim. Acta*, (submitted).

Fogel R.A., Hess P.C. and Rutherford M.J. (1989) Intensive parameters of enstatite chondrite metamorphism. *Geochim. Cosmochim. Acta*, **53**, 2735-2746.

Fredriksson K. and Henderson E.P. (1965) The Horse Creek, Baca County, Colorado, Iron Meteorite. *Trans. Am. Geophys. Union*, **46**, 121.

Gibson E.K., Moore C.B., Primus T.B. and Lewis C.F. (1985) Sulfur in achondritic meteorites. *Meteoritics*, **20**, 503-511.

Goldstein J.I. and Axon H.J. (1973) The Widmanstatten figure in iron meteorites. *Naturwiss.*, **60**, 313-321.

Graham A.L. (1978) Metal and schreibersite in Mayo Belwa, an enstatite achondrite. *Meteoritics*, **13**, 235-244.

Graham A.L. and Henderson P. (1985) Rare earth element abundances in separated phases of Mayo Belwa, an enstatite achondrite. *Meteoritics*, **20**, 141-149.

Herbert F. and Sonnet C.P. (1979) Electromagnetic heating of minor planets in the early solar system. *Icarus*, **40**, 484-496.

Irving A.J. (1978) A review of experimental studies of crystal/liquid trace element partitioning. *Geochim. Cosmochim. Acta*, **42**, 743-770.

Jones J.H. and Drake M.J. (1983) Experimental investigations of trace element fractionation in iron meteorites, II: The influence of sulfur. *Geochim. Cosmochim. Acta*, **47**, 1199-1209.

Jones J.H. and Drake M.J. (1986) Geochemical constraints on core formation in the Earth. *Nature*, **322**, 221-228.

Keil K. (1968) Mineralogical and chemical relationships among enstatite chondrites. *J. Geophys. Res.*, **73**, 6945-6976.

Keil K. (1989) Enstatite meteorites and their parent bodies. *Meteoritics*, **24**, 195-208.

Keil K. and Brett R. (1974) Heideite, a new mineral in the Bustee enstatite achondrite. *Am. Mineral.*, **59**, 465-470.

Keil K. and Fredriksson K. (1963) Electron microprobe analysis of some rare minerals in the Norton County achondrite. *Geochim. Cosmochim. Acta*, **27**, 939-947.

Keil K., Ntaflos Th., Taylor G.J., Brearley A.J., Newsom H.E. and Romig Jr. A.D. (1989) The Shallowater aubrite: evidence for origin by planetesimal impacts. *Geochim. Cosmochim. Acta*, **53**, 3291-3307.

Kelly W.R. and Larimer J.W. (1977) Chemical fractionations in meteorites - VIII. Iron meteorites and the cosmochemical history of the metal phase. *Geochim. Cosmochim. Acta*, **41**, 93-111.

Kruse H. (1979) Spectra processing with computer graphics. Proc. Conf. Computers in Activation Analysis and Gamma-Ray Spectroscopy, Mayaquez, Puerto Rico, p. 76-84.

Kruse H. and Spettel B. (1982) A combined set of automated and interactive programs for instrumental neutron activation analysis. *J. Rad. Chem.*, **70**, 427-434.

Kubaschewski O. (1982) Iron - Binary phase diagrams. Springer-Verlag. 185 pp.

Larimer J.W. and Buseck P.R. (1974) Equilibration temperatures in enstatite chondrites. *Geochim. Cosmochim. Acta*, **38**, 471-477.

Mayeda T.K. and Clayton R.N. (1980) Oxygen isotopic compositions of aubrites and some unique meteorites. *Proc. Lunar Planet. Sci. Conf.*, **11th**, 1145-1151.

McCall G.J.H. (1965) A meteorite of unique type from Western Australia: The Mount Egerton stony-iron. *Mineral. Mag.*, **35**, 241-249.

Mittlefehldt D.W. (1990) Petrogenesis of mesosiderites: I. Origin of mafic lithologies and comparison with basaltic achondrites. *Geochim. Cosmochim. Acta*, **54**, 1165-1173.

Newsom H.E. (1986) Constraints on the origin of the Moon from the abundance of molybdenum and other siderophile elements. In Origin of the Moon (Hartman, W.K., Phillips, R.J., and Taylor G.J., eds.). Lunar and Planetary Institute, Houston. pp. 203-219.

Newsom H.E. and Drake M.J. (1979) The origin of metal clasts in the Bencubbin meteoritic breccia. *Geochim. Cosmochim. Acta*, **43**, 689-707.

Ntaflos Th., Keil K. and Newsom H.E. (1988) Khor Temiki: an enstatite achondrite with evidence of mixing of metal and sulfides from separate sources. *Lunar Planet. Sci.*, **XIX**, 870-871.

Okada A., Tetsuzo I., Kobayashi K. and Sakurai T. (1987) Crystal structure of perryite. *12th Symp. Antarct. Meteorites*, 76.

Okada A., Keil K., Taylor G.J. and Newsom H.E. (1988) Igneous history of the aubrite parent asteroid: evidence from the Norton County enstatite achondrite. *Meteoritics*, **23**, 59-74.

Palme H. and Rammensee W. (1981) The significance of W in planetary differentiation processes: evidence from new data on eucrites. *Proc. Lunar Planet. Sci. Conf.*, **12B**, 949-964.

Palme H., Wlotzka F., Spettel B., Dreibus G. and Weber H. (1988) Camel Donga: A eucrite with high metal content. *Meteoritics*, **23**, 49-57.

Ramdohr P. (1963) The opaque minerals in stony meteorites. *J. Geophys. Res.*, **68**, 2011-2036.

Ramdohr P. (1973) The Opaque Minerals in Stony Meteorites. Elsevier, 245 pp.

Rammensee W. and Wanke H. (1977) On the partition coefficient of tungsten between metal and silicate and its bearing on the origin of the Moon. *Proc. Lunar Planet. Sci. Conf.*, **8th**, 399-409.

Raynor G.V. and Rivlin V.G. (1985) Critical evaluation of cobalt-iron-silicon and iron-nickel-silicon alloys. *Int. Metals Rev.*, **30**, 181-208.

Richter G.R., Wolf R. and Anders E. (1979) Aubrites: are they direct nebular condensates? *Lunar Planet. Sci.*, **X**, 1028-1030.

Robie R.A., Hemingway B.S. and Fisher J.R. (1978) Thermodynamic properties of minerals and related substances at 298.15 °K and 1 Bar (10^5 Pascals) pressure and at higher temperatures. *U.S. Geol. Surv. Bull.*, No. **1452**.

Rubin A.E. (1983) Impact melt-rock clasts in the Hvittis enstatite chondrite breccia: implications for a genetic relationship between EL chondrites and aubrites. *Proc. Lunar Planet. Sci. Conf.*, **14th**, *J. Geophys. Res.*, **89**, B293-B300.

Saikumar V. and Goldstein J.I. (1988) An evaluation of the methods to determine the cooling rates of iron meteorites. *Geochim. Cosmochim. Acta*, **52**, 715-726.

Sakao H. and Elliot J.F. (1975) Thermodynamics of dilute b.c.c. iron-silicon alloys. *Metall. Trans.*, **6A**, 1849-1851.

Schmitt W., Palme H. and Wanke H. (1989) Experimental determination of metal/silicate partition coefficients for P, Co, Ni, Cu, Ga, Ge, Mo and W and some implications for the early evolution of the Earth. *Geochim. Cosmochim. Acta*, **53**, 173-185.

Sears D.W. (1980) Formation of E chondrites and aubrites - A thermodynamic model. *Icarus*, **43**, 184-202.

Seybolt A.U. (1958) Studies on the metallurgy of silicon-iron: 1- Silicon nitrides. 2- Anomaly in the alpha solid solution. *Trans. Metall. Soc. AIME*, **212**, 161-167.

Stoffler D., Bischoff A., Buchwald V. and Rubin A.E. (1988) Shock effects in meteorites. In: Meteorites and the Early Solar System (Kerridge J.F. and Matthews M.S., eds.). University of Arizona Press, pp. 165-202.

Taylor G.J. (1989) Metal segregation in asteroids. *Lunar Planet. Sci.*, **XX**, 1109-1110.

Wai C.M. (1970) The metal phase of Horse Creek, Mount Egerton and Norton County enstatitic meteorites. *Mineral. Mag.*, **37**, 905-908.

Wai C.M. (1974) Geochemical affinities of cobalt and germanium toward metal, silicate, and sulfide phases at high temperature. *Geochim. Cosmochim. Acta*, **38**, 1821-1825.

Wai C.M. and Wasson J.T. (1969) Silicon concentrations in the metal of iron meteorites. *Geochim. Cosmochim. Acta*, **33**, 1465-1471.

Wai C.M. and Wasson J.T. (1970) Silicon in the Nedagolla ataxite and the relationship between Si and Cr in reduced iron meteorites. *Geochim. Cosmochim. Acta*, **34**, 408-410.

Wasson J.T. (1985) Meteorites. Their Record of Early Solar-System History. W.H. Freeman and Co., 267 pp.

Wasson J.T. and Wai C.M. (1970) Composition of metal, schreibersite and perryite of enstatite achondrites and the origin of enstatite chondrites and achondrites. *Geochim. Cosmochim. Acta*, **34**, 169-184.

Watters T.R. and Prinz M. (1979) Aubrites: their origin and relationship to enstatite chondrites. *Proc. Lunar Planet. Sci. Conf.,* **10th**, 1073-1093.

Watters T.R. and Prinz M. (1980) Mt. Egerton and the aubrite parent body. *Lunar Planet. Sci.*, **XI**, 1225-1227.

Wheelock M.M. (1990) Magmatic history of an aubrite body: evidence from igneous clasts and trace elements. M.Sc. Thesis. University of New Mexico, 80 pp.

Wheelock M.M., Heavilon C.F., Keil K., Taylor G.J. and Crozaz G. (1989) Coarse-grained oldhamite in an igneous clast in the Norton County aubrite: REE measurements. *Meteoritics*, **24**, 340-341.

Willis J. and Goldstein J.I. (1981) A revision of metallographic cooling rate curves for chondrites. *Proc. Lunar Planet. Sci. Conf.*, **12B**, 1135-1143.

Wolf R., Ebihara M., Richter G.R. and Anders E. (1983) Aubrites and diogenites: trace element clues to their origins. *Geochim. Cosmochim. Acta*, **47**, 2257-2270.

Wood J.A. (1967) Chondrites: Their metallic minerals, thermal histories, and parent planets. *Icarus*, **6**, 1-49.

8104208